Summer 8-2023

Performance and Emissions Study of N+3 and N+4 Engine Models with Several Fuel types Using NPSS

Abel Solomon
Washington University in St. Louis

WASHINGTON UNIVERSITY IN ST. LOUIS

McKelvey School of Engineering
Department of Mechanical Engineering & Materials Science

Thesis Examination Committee
Ramesh Agarwal, Chair
Swami Karunamoorthy
Xianglin Li

Performance and Emissions Study of N+3 and N+4 Engine Models with Several Fuel types Using NPSS

by

Abel Solomon

A thesis presented to
the McKelvey School of Engineering
of Washington University in
partial fulfillment of the
requirements for the degree
of Master of Science

August 2023
St. Louis, Missouri

Table of Contents

List of Figures iv
List of Tables v
Acknowledgments vi
Abstract viii
Chapter 1: Motivation and Introduction 1
1.1 Motivation 1
1.2 Introduction 2
1.2.1 N+3 and N+4 Technology Level Turbofan Engines 2
1.2.2 Numerical Propulsion System Simulation (NPSS) 3
1.3 Scope of Thesis 3
1.4 References 5
Chapter 2: Choice of Alternative Fuels 6
2.1 Liquid Hydrogen (LH_2) 6
2.3 Ammonia Cracking (NH_3) 7
2.4 Ammonia Borane (BH_3NH_3 or AB) 8
2.5 Liquefied Natural Gas (LNG) 9
2.6 References 10
Chapter 3: NPSS Code Development for N+3 and N+4 Engines 12
3.1 NPSS Development 12
3.2 Propulsion System Equations 15
3.3 References 18
Chapter 4: Study of the Effect of Bypass Ratio on Thrust Specific Fuel Consumption 19
4.1 Introduction 19
4.2 Method 19
4.3 Results 22
4.4 Conclusion 27
4.5 References 28
Chapter 5: Performance Study of N+3 Turbofan Engine Model with Several Types of Fuels Using NPSS 29

5.1 Introduction 29
5.2 Method 30
5.3 Results 31
5.4 Conclusion 33
5.5 References 34
Chapter 6: Emission studies of N+3 and N+4 Technology Level Propulsion Systems with Alternative Fuels 36
6.1 Introduction 36
6.2 Methods 36
6.3 Results 40
6.4 Conclusion 46
6.5 References 47
Chapter 7: Summary 49
Appendix A: MATLAB Code ..... [51]
3rd order Polynomial Fit Sample Code and Data ..... [54]
Appendix B: Initial Estimates ..... [55]
Appendix C: Example NPSS Input File ..... [56]

List of Figures

Figure 1: Schematic of a double a double spool geared turbofan engine representative of the NASA N+3 and N+4 engine models. 14

Figure 2: Screenshot of the command prompt window showing NPSS Solver dependent and independent variables..... 21

Figure 3: Sample screenshots of the viewOut file obtained from NPPS 23

Figure 4: TSFC vs. FPR (primary axis) and BPR vs. FPR (secondary axis) for Jet-A fuel. The linear fit is placed to show the increasing or decreasing trend of the plot. The plots can be fitted well using a polynomial fit of degree 3 (see Appendix A for detail). 24

Figure 5: TSFC vs. FPR (primary axis) and BPR vs. FPR (secondary axis) for LH_2 fuel. The linear fit is placed to show the increasing or decreasing trend of the plot. The plots can be fitted well using a polynomial fit of degree 3 (see Appendix A for detail). 25

Figure 6: Plot showing the effect of increasing BPR on TSFC using Jet-A as a fuel source. 26

Figure 7: TSFC vs BPR plot comparing the results obtained from MATLAB and NPSS using the fixed core method. 32

Figure 8: TSFC vs BPR plot comparing the performance of three types of fuels in NPSS: conventional Jet-A, Ammonia (NH3), and Liquid Hydrogen (LH2). 33

List of Tables

Table 1: H_2 release temperature points during thermal decomposition of NH_3 and BH_3NH_3..... 8

Table 2: Properties associated with Jet-A, liquified natural gas (LNG), liquid hydrogen (LH_2), ammonia (NH_3), ammonia cracking, and thermal decomposition of Ammonia borane (AB). 10

Table 3: Performance parameters for NASA N+3 and N+4 high bypass geared turbofan engine models. 13

Table 4: Dependent and independent variables used for NPSS solver setup. 30

Table 5: Emissions Indexes for Jet-A. 37

Table 6: Emissions Indexes for Liquid Hydrogen (LH2). 37

Table 7: Elementary reaction steps for combustion of Liquid Hydrogen (LH2) [5]. 38

Table 8: Elementary reaction steps for combustion of Ammonia (NH3) [4]. 39

Table 9: Performance and emissions comparison between Jet-A, LH2, and NH3 for N+3 engine model..... 41

Table 10: Performance and emissions comparison between Jet-A, NH3 cracking, and thermal decomposition of AB for N+3 engine model..... 42

Table 11: Performance and emissions comparison between Jet-A and LNG for N+3 engine model..... 43

Table 12: Performance and emissions comparison between Jet-A, LH2, and NH3 for N+4 engine model..... 44

Table 13: Performance and emissions comparison between Jet-A, NH3 cracking, and thermal decomposition of AB for N+4 engine model..... 45

Table 14: Performance and emissions comparison between Jet-A and LNG for N+4 engine model..... 46

Table 15: Coefficients of the 3rd order polynomial fit 54

Acknowledgments

My deepest gratitude goes to Dr. Ramesh Agarwal for his unwavering support and guidance. I would like to thank Richard Carter for helping me get familiarized with NPSS. Thanks to the committee members Dr. Li and Dr. Karunamoorthy for reading the thesis and attending its defense. Finally, thanks to everyone from CFD lab for their comradery and friendship.

Abel Solomon

Washington University in St. Louis

August 2023

Dedicated to my family

ABSTRACT OF THE THESIS

Performance and Emissions Study of N+3 and N+4 Engine Model with Several Fuel types Using NPSS

by

Abel Solomon

Master of Science in Mechanical Engineering

Washington University in St. Louis, 2023

Professor Ramesh Agarwal, Chair

The aviation industry is known to be one of the major contributors to greenhouse gases accounting for 4.9% of the global greenhouse emissions. With the ever-increasing threat of climate change to the overall survival of the planet, the exploration of new technologies and alternative energy sources that minimize greenhouse gas emissions are of paramount importance. In this regard, the development of propulsion systems well suited for performance and emissions requirements of future commercial aircrafts plays a crucial role. This thesis investigates N+3 and N+4 technology level propulsion systems that are proposed by NASA as a possible propulsion system for an advanced single-aisle commercial aircraft. Numerical simulation is utilized to evaluate the performance and emissions associated with the engines. The simulation is performed on the software called NPSS which is a component based object-oriented engine cycle analysis and simulation tool. Liquid hydrogen (LH2), liquefied natural gas (LNG), ammonia (NH3), and ammonia-borane (AB) are explored as alternative fuel sources alternative to the conventional Jet-A fuel.

The engine size is fixed using published reference data from NASA and a fixed core engine model is developed and validated against the results obtained from fundamental

propulsion equations coded in MATLAB; good agreement is obtained (with in $\pm 8\%$) for variation in Thrust Specific Fuel Consumption (TSFC) with Bypass Ratio (BPR). After validation of the NPSS engine model, a BPR sensitivity study is performed and the result shows that there is a significant improvement in TSFC with increasing BPR. To reduce the effect of the undesirable consequence of increasing drag with BPR, it is crucial to find the optimal BPR level and The BPR sensitivity study presented in this thesis can be used as a starting point in sizing an engine during design process. Although the emissions study presented in this paper uses indexes, having robust models that can accurately predict emissions associated with alternative fuels is essential for the acceleration of technology development and implementation. In the absence of experimental data, the results presented in this work can be used as a reference for future attempts to enhance the accuracy of the emissions estimation.

Chapter 1: Motivation and Introduction

This chapter presents the motivation behind the research presented in this thesis. A brief introduction to Numerical Propulsion System Simulation (NPSS) software is given. Basic working principles of the N+3 and N+4 technology level turbofan engines are discussed. Lastly, the scope of the thesis is presented as it appears in the consecutive chapters.

1.1 Motivation

The effect of global warming and its associated impact on climate change necessitate the urgent need for multi-faceted solutions for the planet to be saved from disastrous consequences. The main contributors to global warming are the release of greenhouse gases such as carbon dioxide (CO_2), methane (CH_4), water vapor (H_2O) and other particulates into the atmosphere through the burning of fossil fuels [1]. In comparison to other greenhouse gases, CO_2 emission is by far the largest contributor to the global warming accounting for 76% of the global greenhouse gas emissions [2]. The global aviation industry alone contributes about 2.1% of the global CO_2 emissions, and when included with other greenhouse gases, it accounts for 4.9% making it a significant contributor to global warming [3]. Therefore, the need for a cleaner fuel energy source for aviation to achieve a zero-emission future is apparent.

In recent years, the aviation industry therefore is increasingly focused on exploring alternative energy sources (fuels) that can reduce the environmental impact of its current carbon emissions due to combustion of Jet-A fuel [4]. One way to accomplish this goal is to explore propulsion technologies that support alternative fuels which have reduced or zero-carbon emissions such as hydrogen or ammonia among others. For regional travel distances of 1000

nautical miles or less, the current advancement in battery and fuel cell technology have made it possible to create propulsion systems with zero emissions assuming that the fuel used for fuel-cell (namely the hydrogen) is obtained from sustainable sources such as solar, wind, or nuclear energy [5]. However, the application of such technologies is limited to short-haul flights; the gas turbine combustion remains the only viable option for long distance air transportation of greater than 1000 nautical miles which covers about 70% of the world air traffic. In this regard, sustainable aviation fuels (SAFs) and non-hydrocarbon fuels such as liquid hydrogen (LH2), Ammonia (NH_3), and Ammonia Borane (AB) are promising alternatives to the Jet-A fuel currently in use. This study aims to evaluate the performance of these alternative fuels by conducting numerical investigation of propulsion and associated emissions using NPSS. The engine models explored in this numerical investigation are N+3 and N+4 technology level high bypass geared turbofan engines.

1.2 Introduction

1.2.1 N+3 and N+4 Technology Level Turbofan Engines

To achieve the ambitious goals of the emission free next generation of aircrafts, development of new propulsion systems is imperative. N+3 and N+4 technology level turbofan engines are advanced propulsion systems that are being developed by the aerospace industry to meet the growing demand for more efficient and environmentally friendly aircrafts while advancing in operational capability [6, 7]. The terms N+3 and N+4 refer to the third and the fourth generation of engine technologies, respectively. In addition to improving the overall engine performance and reliability, this new generation of propulsion systems are expected to reduce fuel consumption by about 30%, reduce carbon emission by about 70%, and reduce noise by about 65% compared to current technology levels. The advancement of new technologies

such as N+3 and N+4 propulsion systems are of paramount importance in the development of aircrafts that are environmentally friendly, efficient, and cost effective.

1.2.2 Numerical Propulsion System Simulation (NPSS)

Numerical Propulsion System Simulation (NPSS) is a component based object-oriented engine cycle analysis and simulation tool. It was originally developed by NASA Glenn Research Center to be used for the creation, study and sharing of complete aerothermal-mechanical computer simulations of propulsion systems [8]. In NPSS, the model definitions are given through input files. The software has a set of modules that correspond to the different components of a gas turbine engine such as fan, compressor, burner, turbine, and nozzles. A complete engine model can be created by combining the individual modules. The simulation system also has a built-in NIST compliant gas property packages to perform different thermochemistry simulations. NPSS has sophisticated solver with auto-setup, constraints, and discontinuity handling. The object-oriented design of NPSS facilitates user-definable elements, functions, and models. There are several published engine cycle data sets on NASA's website, including N+3 and N+4 engine cycle data [6, 7], which can be utilized to model an engine in NPSS.

1.3 Scope of Thesis

The goal of this research is to explore alternative fuel sources that are capable of supplying the required power level while minimizing emissions. The alternative fuels considered are LH_2, NH_3, AB, and LNG. Numerical simulation is utilized to quantify emissions and propulsive efficiencies of both N+3 and N+4 technology level propulsion systems. The simulation is executed using NPSS.

Chapter 2: Choice of Alternative Fuels: In this chapter, the alternative fuels investigated in this thesis are presented. The reasoning behind the choice of alternative fuels is discussed.

Chapter 3: NPSS Code Development for N+3 and N+4 Engine Designs: This chapter explains the development and validation procedures of the NPSS code for the N+3 and N+4 representative engine models. The engines design parameter as well as equations used for performance evaluation are discussed in detail.

Chapter 4: Validation of NPSS: In this chapter, the validation of the NPSS code against results from a MATLAB code is discussed. The main aim of this chapter is to investigate the capability of NPSS to model and size a rubber engine and produce expected results from rudimentary propulsive performance calculations.

Chapter 5: Performance Study of N+3 Turbofan Engine Model with Several Types of Fuels Using NPSS: In this chapter, the performance of a fixed core propulsive system representative of N+3 engine model is evaluated. A bypass ratio (BPR) sensitivity study on the engine, quantified by the thrust specific fuel consumption (TSFC), is discussed and the significance of the results is presented.

Chapter 6: Emission studies of N+3 and N+4 Technology Level Propulsion Systems with Alternative Fuels: A detailed description of the emissions calculation method and performance comparisons among Jet-A, liquefied natural gas (LNG), liquid hydrogen (LH_2), ammonia (NH_3), and ammonia-borane (AB) are presented in this chapter. General cruise cycle data is presented to aid in further research efforts of aircraft and propulsion system designs that take emissions into account.

Chapter 7: Summary: This chapter summarizes the main findings of the research. Recommendations based on the findings and future directions are discussed briefly.

1.4 References

[1] Melissa Denchak, “Greenhouse Effect 101.” https://www.nrdc.org/stories/greenhouse-effect-101#:~:text=The%20main%20gases%20responsible%20for,gases%20(which%20are%20synthetic).

[2] O. US EPA, “Global Greenhouse Gas Emissions Data,” Jan. 12, 2016. https://www.epa.gov/ghgemissions/global-greenhouse-gas-emissions-data (accessed Sep. 08, 2022).

[3] “156_CAN ICSA Aviation TD submission.pdf.”

[4] R. E. Carter and R. K. Agarwal, “Development of a Liquid Hydrogen Combustion High Bypass Geared Turbofan Model in NPSS,”AIAA Paper 2022-3431, in AIAA Aviation 2022 Forum, Chicago, IL, 27 June - 1 July 2022, doi: 10.2514/6.2022-3431.

[5] “Forum 360: Hydrogen: Hope or Hype?,” https://www.aiaa.org/detail/session/pe-forum-360-2-11aug21 (accessed Apr. 08, 2023).

[6] S. M. Jones, W. J. Haller, and M. T.-H. Tong, “An N+3 Technology Level Reference Propulsion System,” E-19373, May 2017. Accessed: Apr. 08, 2023. [Online]. Available: https://ntrs.nasa.gov/citations/20170005426

[7] M. K. Bradley and C. K. Droney, “Subsonic Ultra Green Aircraft Research Phase II: N+4 Advanced Concept Development,” NF1676L-14434, May 2012. Accessed: Apr. 08, 2023. [Online]. Available: https://ntrs.nasa.gov/citations/20120009038

[8] Charles Krouse, “Introduction to Propulsion Simulation Using NPSS.” Southwest Research Institute, 2021.

Chapter 2: Choice of Alternative Fuels

Conventional Jet-A fuel is the commonly used energy source for both commercial and military aircrafts. It is a kerosene-based aviation fuel with enhanced qualities of low freezing point and high flash point which makes it ideal for use in aviation [1]. Although Jet-A meets the current safety, performance, and environmental regulations, it is not suitable for future generations of aircrafts that would have to meet much more strict environmental regulations and performance requirements. Since Jet-A is kerosene-based fuel it is in fact a fossil fuel and has a negative impact on the environment including greenhouse gas emissions. At the moment, Jet-A is the standard aviation fuel every airport supplies, thus the explorations of alternative fuel sources to the conventional Jet-A fuel should be the first steep to reduce the environmental impact of air transport. The alternative fuels explored in this research are liquid hydrogen (LH_2), liquid natural gas (LNG), ammonia (NH_3), and ammonia borane (BH_3NH_3 or AB). The advantages and disadvantages of each fuel are discussed below.

2.1 Liquid Hydrogen (LH_2)

Liquid hydrogen is a promising candidate for aviation fuel due to its high energy content per unit of mass. The lower heating value (LHV) of liquid hydrogen is about 51,590 BTU/lbm which is significantly higher than the LHV value of conventional Jet-A fuel which is around 18,500 BTU/lbm. However, there are downsides associated with the use of liquid hydrogen, primarily in storage, transportation, and volume requirements. Due to the extremely low boiling point of hydrogen (-252.9^{o}C), it must be stored in a cryogenic tank at a very high pressure to keep it in liquid form, and this requires significant amount of energy. Moreover, since liquid hydrogen has very low density, the fuel tank volume requirement is considerably higher than that

of conventional Jet-A fuel. Although the stoichiometric equation for LH_2 combustion reaction (with air) shown in Eq.1 produces only N_2 and H_2O as byproducts [2], at elevated temperatures the combustion can result in the production of NO_x which is the primary contributor to acid rain [3].

$$2H_2 + 7.546N_2 + O_2 \rightarrow 3.774N_2 + 2H_2O \quad (1)$$

2.2 Ammonia (NH_3)

The use of ammonia as an aviation fuel has gained interest in recent years due to its low greenhouse gas emission with only NO_x as the product of its combustion. In addition, the production of ammonia can be carbon-neutral or even carbon-negative depending on how it is sourced and the energy used to produce it. It can be produced easily from biomass using renewable energy sources. The storage and transportation of ammonia is rudimentary and does not require much energy as compared to liquid hydrogen. However, it has a very low LHV value of 7,996 BTU/lbm which implies a larger fuel tank, just as in the case of liquid hydrogen, and more fuel mass is required. Despite these challenges, ammonia has the potential to be used as an environmentally friendly aviation fuel. Equation 2 shows the stoichiometric combustion reaction of ammonia with air [4]. The formation of NO_x is seen at elevated temperature combustion.

$$2NH_3 + 5.64N_2 + 1.5O_2 \rightarrow 6.64N_2 + 3H_2O \quad (2)$$

2.3 Ammonia Cracking (NH_3)

Instead of using ammonia as an aviation fuel directly, it can be cracked catalytically or via a plasma reactor to extract the hydrogen [5]. Essentially, ammonia is considered to be a hydrogen carrier in this application. The high density (~0.6 kg/L) and high hydrogen content by mass (~17.65 %) of ammonia makes possible to store more hydrogen per volume of fuel as

compared to pure liquid hydrogen [6]. The drawback of ammonia cracking is the needed for complicated auxiliary units required for cracking ammonia on board and the associated extra energy cost. For the purpose of this study, hydrogen is assumed to be cracked off of ammonia, whether it is catalytically or via a plasma reactor, prior to being injected into the combustion chamber. Thus, hydrogen is assumed as a fuel for combustion; however, the LHV value is adjusted by considering the density of ammonia [7].

2.4 Ammonia Borane (BH_3NH_3 or AB)

Ammonia borane is another alternative fuel for use as a hydrogen carrier to overcome the problematic and expensive requirements of hydrogen storage and transportation. It has higher hydrogen content by mass releasing about 19.6 wt.% of hydrogen as can be seen in Eq. 3 [8]. Ammonia Borane is solid at standard room temperature and pressure and although the decomposition of hydrogen is possible at solid-state, it cannot be used as a fuel for aircraft engines as they require liquid fuels. Also, combusting ammonia borane at the turbine inlet temperature of a representative turbofan engine can lead to crystalline products creating issues for turbine life and performance. Thus, just as in the case of ammonia cracking, the dehydrogenation of ammonia borane can be induced via catalysts or through thermal decomposition to produced injectable hydrogen. The thermal decomposition of Ammonia and Ammonia Borane occurs at temperatures much cooler than in a typical turbine engine combustor as shown in Table 1 which make this a potential option [4, 7].

$$BH_3NH_3 \rightarrow BN + 3H_2 \tag{3}$$

Table 1: H_2 release temperature points during thermal decomposition of NH_3 and BH_3NH_3.

Thermal Decomposition	Ammonia NH3 [R]	Ammonia Borane BH_3NH_3 [R]

Temps		
1st H_2	2471.7	689.7
2nd H_2	NA	725.7
3rd H_2	NA	2651.7

2.5 Liquefied Natural Gas (LNG)

LNG is advertised as the "cleanest fossil fuel" because it is primarily made up of methane (CH_4). The combustion of LNG produces less soot and generates 30% less carbon dioxide than oil fuel and a 50% decrease in NOx production [9]. In addition, LNG has LHV of around 21,000 BTU/lbm [10] which is higher than that of Jet-A fuel. The stoichiometric reaction for the combustion of LNG in air is given by Eq. (4) [11]. For the purpose of this study, since greater than 90% of LNG is methane, methane is used as a fuel when modeling the propulsion in NPSS with the LHV value of LNG.

$$CH_4 + 2O_2 + 7.53N_2 \rightarrow CO_2 + H_2O + 7.53N_2 \quad (4)$$

Table 2 summarizes the energy content of the fuels used in this research. Note that the LHV values for NH_3 cracking and BH_3NH_3 thermal decomposition reflect the LHV value of hydrogen adjusted with its wt.% in each fuel.

Table 2: Properties associated with Jet-A, liquefied natural gas (LNG), liquid hydrogen (LH_2), ammonia (NH_3), ammonia cracking, and thermal decomposition of Ammonia borane (AB).

	Molar Mass [g/mol]	LHV [MJ/kg]	LHV [BTU/lbm]	Density [kg/L]	Volumetric LHV [MJ/L]	Molar LHV [MJ/mol]	Flash Pt [R]	Auto Ignition Temp [R]
Jet A	~158.6	43.1	18,530	0.8	34.480	6.836	560.1	870
LNG	~18.1	50.2	20,894	0.45	22.59	0.9086	NA	1570
LH_2	2.01588	120	51,591	0.0708	8.496	0.242	36	1455
NH_3	17.0305	18.6	7,996	0.604	11.234	0.317	729.3	1663
NH_3 Cracking	17.0305	21.3*	9,157*	0.604	12.865*	0.363*	36*	1455*
Thermal Decomp. of BH_3NH_3	30.86534	15.7*	6,739*	0.78	12.226*	0.484*	36*	1455*

*values derived from corresponding LH_2 values

2.6 References

[1] "Aviation Fuels: Jet Fuel, Aviation Gasoline (Avgas), Jet B, Biokerosene," *Oiltanking*. https://www.oiltanking.com/en/news-info/glossary/aviation-fuels-jet-fuel-aviation-gasoline-avgas-jet-b-biokerosene.html (accessed Apr. 08, 2023).

[2] HySafe - Safety of Hydrogen as an energy Carrier, "HYDROGEN THERMOCHEMISTRY: Fundamentals of Hydrogen Safety." [Online]. Available: http://www.hysafe.org/img/fhslect03.pdf

[3] A study by the Department of Energy, "Hydrogen Use in Internal Combustion Engines." College of the Desert, Palm Desert, CA, Dec. 2001. [Online]. Available: https://www1.eere.energy.gov/hydrogenandfuelcells/tech_validation/pdfs/fcm03r0.pdf

[4] R. Khamedov, W. Song, F. E. Hernandez Perez, and H. G. Im, "A Computational Study of Ammonia Combustion in MILD Conditions," AIAA Paper 2021-0798, in AIAA SciTech 2021 Virtual Forum, doi: 10.2514/6.2021-0798.

[5] J. Brandenburg, "Plasma Reactor for Ammonia Cracking to Hydrogen," UCF Patent, May 2006, [Online]. Available: https://stars.library.ucf.edu/patents/460

[6] George Thomas and George Parks, "Potential Roles of Ammonia in a Hydrogen Economy." U.S. Department of Energy, Feb. 2006. [Online]. Available:

https://www.energy.gov/eere/fuelcells/articles/potential-roles-ammonia-hydrogen-economy#:~:text=Second%2C%20ammonia%20has%20a%20large,of%20the%20mass%20of%20ammonia.

[7] D. Himmelberger, “Hydrogen Release From Ammonia Borane,” Publicly Access. Penn Diss., May 2010, [Online]. Available: https://repository.upenn.edu/edissertations/158

[8] S. Akbayrak and S. Özkar, “Ammonia Borane as Hydrogen Storage Materials,” Int. J. Hydrog. Energy, Vol. 43, No. 40, pp. 18592–18606, Oct. 2018, doi: 10.1016/j.ijhydene.2018.02.190.

[9] “Can Aviation Use Liquefied Natural Gas To Reduce Its Carbon Footprint? | Aviation Week Network.” https://aviationweek.com/air-transport/aircraft-propulsion/can-aviation-use-liquified-natural-gas-reduce-its-carbon (accessed Dec. 02, 2022).

[10] “Fuels - Higher and Lower Calorific Values.” https://www.engineeringtoolbox.com/fuels-higher-calorific-values-d_169.html (accessed Dec. 02, 2022).

[11] “What is the Air Fuel Ratio Effect on Combustion Efficiency?” https://sagemetering.com/combustion-efficiency/air-fuel-ratio-effect-on-combustion-efficiency/ (accessed Dec. 02, 2022).

Chapter 3: NPSS Code Development for N+3 and N+4 Engines

3.1 NPSS Development

Turbofan engines can achieve higher thrust level with lower fuel consumption compared to turbojet engines by utilizing some of the energy produced by the turbine to drive a fan. The fan draws large amount of air into the engine and thus yields higher thrust per unit amount of fuel used. One can increase the size of the fan to get lower Thrust Specific Fuel Consumption (TSFC) value. However, increasing the size of fan creates aerodynamic issues since the drag force would increase. Hence, modern turbofan engines are designed to achieve lower TSFC values while keeping the aerodynamic drag created by a larger fan as low as possible.

The next generation of propulsion systems is designed to eliminate some of the drawbacks of the current turbofan engines such as noise, fuel efficiency, and most importantly emissions. N+3 and N+4 propulsion systems have been proposed to do just that. Table 3 shows the performance parameters for N+3 and N+4 engines as published by NASA [1, 2]. The current turbofan engines in use are not suited for use with the various alternative fuels discussed in chapter 2. N+3 and N+4 propulsion systems are expected to introduce new engine architectures that are capable of running on these new fuels.

Table 3: Performance parameters for NASA N+3 and N+4 high bypass geared turbofan engine models

Propulsion System Parameters	**NASA N+3 Technology Level Reference Propulsion System**	**NASA N+4 Concept Vehicle Propulsion System: gFan++ Advanced Turbofan (JP+2045GT+DF)**
Fan Diameter [in]	100	71.4
Propulsion System Wt. [lbm]	9300	6379
SLS Thrust [lbf]	28620.8	21943
SLS SFC [lbm/lbf/hr.]	0.1751	0.214
RTO Thrust [lbf]	22800	16592
RTO SFC [lbm/lbf/hr.]	0.2891	0.286
TOC Thrust [lbf]	6073.2	3931
TOC SFC [lbm/lbf/hr.]	0.4636	0.453
CRZ Thrust [lbf]	5465.8	3145
CRZ SFC [lbm/lbf/hr.]	0.4644	0.442
Cruise Alt [ft.]	35000	38000
Cruise Mach Number [NA]	0.8	0.7

Figure 1 shows representative schematics of the N+3 and N+4 models proposed by NASA. The major components of N+3 and N+4 turbofan engine models include a fan, a low-pressure compressor (LPC), a high-pressure compressor (HPC), a high-pressure turbine (HPT), and a low-pressure turbine (LPT). The addition of an extra compressor enhances the amount of thrust that can be extracted by burning the same amount of fuel while the added turbine supplies the necessary energy needed to turn the fan and compressor blades.

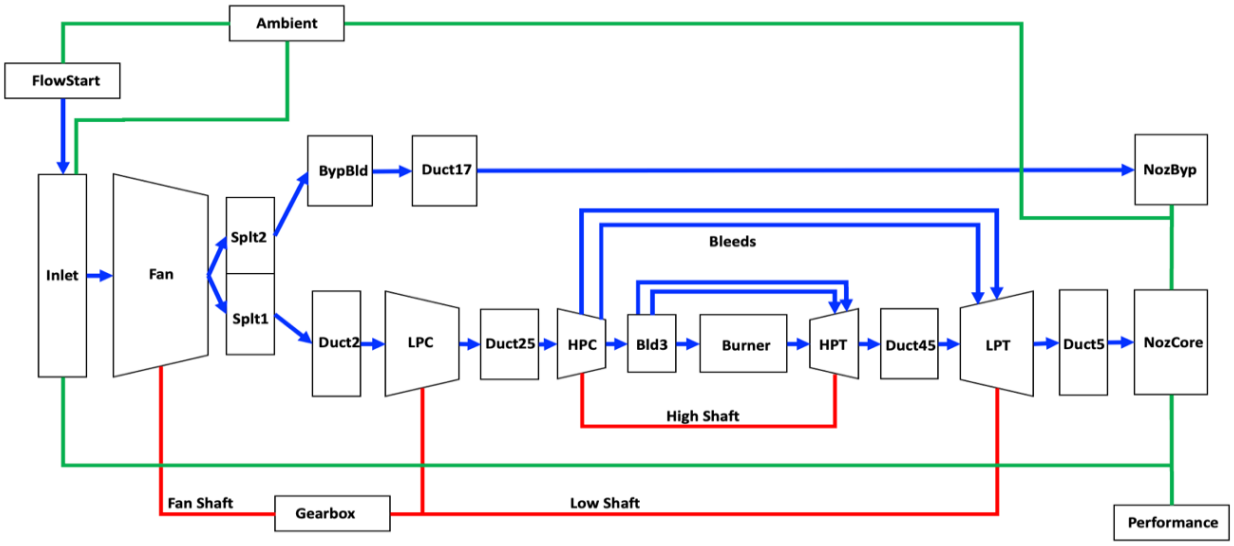

Figure 1: Schematic of a double a double spool geared turbofan engine representative of the NASA N+3 and N+4 engine models.

Numerical Propulsions Systems Simulation (NPSS) software is employed to study the performance and associated emissions of N+3 and N+4 technology level turbofan engines. NPSS is an advanced, object-oriented code written in C++ that is widely used in the industry for modeling thermodynamic propulsion cycles [3]. The code acts as a flow network solver that can simulate all environmental conditions and modes of flight to study the performance of an engine model. In that regard, the N+3 generation high bypass geared turbofan engine cycle was modeled in NPSS based on published NASA engine cycle data [4]. The publicly available published data from NASA include the engine architecture, turbomachinery maps, and technology level material temperatures which were retrieved from NASA's OpenMDAO GitHub repository [1, 5, 6]. As demonstrated by previous studies, NPSS has the capability to simulate propulsion system developed using engine cycle models based on specific performance parameters and publicly available data [4, 7]. The NASA N+3 high bypass technology reference includes several improvements to the architecture based on assumed technology advancements and compressor loading capability. These improvements include a lower fan pressure ratio (1.3), a higher overall

pressure ratio (55), a higher burner outlet temperature (3400^{o}R), and a larger bypass ratio (24) compared to the standard reference CFM 56 [1].

The first step in this study was the development and validation against published performance data of a representative N+3 engine model created using the publicly available engine parameters. To study the performance and emissions of various alternative fuels for N+4 technology level engine, the same model was updated with NASA N+4 performance parameters from Ref. [2]. The NASA N+4 engine report considers multiple advancement options for the propulsion system including designs for Liquefied Natural Gas (LNG), an un-ducted fan (UDF) propulsor, solid oxide fuel cell power plant with UDF, and aft-fuselage mounted ducted turbofans for boundary layer ingestion and wake propulsion [2]. For the purpose of this study, only the original ducted gFan++ Advanced Turbofan propulsion system level requirements were modeled in NPSS. The reference report [2] details the thrust, the thrust specific fuel consumption (TSFC), the compressor and turbine stage numbers, and the compressor pressure ratio values. However, other parameters such as the high-pressure compressor exit pressure and temperature and the high-pressure turbine inlet pressure and temperature are not given. Thus, when modeling the N+4 technology level turbofan engine all the missing information was substituted with N+3 assumptions.

3.2 Propulsion System Equations

The performance of the representative N+3 and N+4 engine models at a single design point can be calculated using basic propulsion equations. According to [8] the thrust force that pushes an aircraft powered by a turbofan engine forward is a result of the flow of air through the

fan and the core. As can be seen from Eq. (1), the net thrust is a combination of the thrust produced by the fan and the thrust produced by the engine core.

$$Net\ Thrust = Thrust\ of\ Fan + Thrust\ of\ Core \tag{1}$$

$$T = (\dot{m}_f v_f - \dot{m}_f v_o) + (\dot{m}_e v_e - \dot{m}_c v_o)$$

where T is thrust in [lbf], $\dot{m}_f$, $\dot{m}_e$, and $\dot{m}_c$ are the mass flow rates at the fan exhaust (connected to the bypass bleed), the core exhaust, and the core inlet, respectively in [lbm/s], v_f, v_o, v_e, are the velocities at the fan exhaust (going to the bypass bleed), the fan entrance (free stream velocity), and the core exhaust, respectively in [ft./s]. The total mass flow of the air is the sum of the mass flow going through the bypass bleed and the mass flow going through the core as can be seen in Eq. (2) below:

$$\dot{m}_o = \dot{m}_f + \dot{m}_c \tag{2}$$

where $\dot{m}_o$ represent the total mass flow of air entering the engine in [lbm/s]. The thrust can be adjusted by changing the size of the core and the bleed. Moreover, the ratio between the fan exhaust mass flow rate to the compressor mass flow rate gives the bypass ratio as given in Eq. (3).

$$BPR = \dot{m}_f / \dot{m}_c \tag{3}$$

Equation (1) can thus be written in terms of *BPR* and $\dot{m}_o$ as shown in Eq. (4):

$$T = (\dot{m}_e v_e - \dot{m}_o v_o) + BPR * \dot{m}_c * v_f \tag{4}$$

The net thrust (T_{net}) can also be expressed in terms of the change in velocity between the free stream and the jet (ΔV) as:

$$T_{net} = \dot{m}\Delta V \tag{5}$$

where $\Delta V = V_{jet} - V_o$

$V_{jet} = M_9 * \alpha$

The $\dot{m}$ in Eq. (5) represents the change in mass of the aircraft overtime. M_9 is the core nozzle exit Mach number and α is the speed of sound calculated using Eq. (6) as:

$$\alpha = \sqrt{\gamma RT} \tag{6}$$

where γ is the adiabatic index (~1.4 for diatomic molecules such as air), R is the universal gas constant (~53.4 ft·lbf/lb·°R for air), and T is the absolute temperature of the air in which the aircraft is flying through. The change in the kinetic energy of the aircraft can be calculated by Eq. (7):

$$\Delta KE = \frac{1}{2}\dot{m}V_{jet}^2 - \frac{1}{2}\dot{m}V_o^2 = \frac{1}{2}\dot{m}\Delta V(2V_o + \Delta V) \tag{7}$$

For a fixed free stream velocityV_o, propulsive efficiency and V_{jet} have an inverse relationship as shown in Eq. (8):

$$\eta_{prop} = \frac{TV_o}{\Delta KE} = \frac{2V_o}{(V_o + V_{jet})} \tag{8}$$

Moreover, the *FPR*, which is the ratio of the fan exit pressure to fan inlet pressure, can be calculated using the nozzle exit Mach number as given in Eq. (9). For the case of an ideal engine, the nozzle exit pressure matches the ambient pressure ($P_\infty = P_1 = P_9$).

$$FPR = \frac{P_2}{P_1} = \frac{P_2}{P_\infty} = \left[1 + \frac{\gamma - 1}{2}M_9^2\right]^{\frac{\gamma}{\gamma - 1}} \tag{9}$$

By solving Eq. (9) for M_9, the nozzle exit Mach number can be expressed in terms of the *FPR* and the fan inlet pressure (P_1) as given in Eq. (10).

$$M_9 = \sqrt{\frac{2(\sqrt[\frac{\gamma}{\gamma-1}]{FPR}-1)}{\gamma-1}} \tag{10}$$

Thus, as *FPR* is increased to a point in an ideal engine, the nozzle exit Mach number M_9, and consecutively V_{jet} increases. This increase in V_{jet} brings about a decrease in the propulsive efficiency as the two are inversely related. The focus of this thesis is to study the performance of the N+3 and N+4 turbofan engine model while altering the *FPR*.

3.3 References

[1] S. M. Jones, W. J. Haller, and M. T.-H. Tong, "An N+3 Technology Level Reference Propulsion System," E-19373, May 2017. Accessed: [Online]. Available: https://ntrs.nasa.gov/citations/20170005426

[2] M. K. Bradley and C. K. Droney, "Subsonic Ultra Green Aircraft Research Phase II: N+4 Advanced Concept Development," NF1676L-14434, May 2012. Accessed: [Online]. Available: https://ntrs.nasa.gov/citations/20120009038

[3] C. Krouse, "Introduction to Propulsion simulation using NPSS." SWRI, 2021.

[4] R. E. Carter and R. K. Agarwal, "Development of a Liquid Hydrogen Combustion High Bypass Geared Turbofan Model in NPSS," AIAA Paper 2022-3431, in AIAA Aviation 2022 Forum, Chicago, IL, 29 June - 1 July 2022,. doi: 10.2514/6.2022-3431.

[5] "Aerospace | Free Full-Text | pyCycle: A Tool for Efficient Optimization of Gas Turbine Engine Cycles." https://www.mdpi.com/2226-4310/6/8/87

[6] "pyCycle/example_cycles/N+3ref at master · OpenMDAO/pyCycle," GitHub. https://github.com/OpenMDAO/pyCycle

[7] R. E. Carter and B. M. Smith, "The Development of an NPSS Engine Cycle Model to Match Engine Cycle Data, Using a Multi-Design-Point Method," AIAA Paper 2021-0876, in AIAA SciTech 2021 Virtual Forum, doi: 10.2514/6.2021-0876.

[8] "Turbofan Thrust." https://www.grc.nasa.gov/www/k-12/airplane/turbfan.html

Chapter 4: Study of the Effect of Bypass Ratio on Thrust Specific Fuel Consumption

4.1 Introduction

NPSS is utilized to study the effect of *BPR* on TSFC and the NPSS results are validated against simulation results obtained using MATLAB. Thrust Specific Fuel Consumption (TSFC) represents the amount of fuel used per unit thrust; lower value of TSFC indicates less fuel is being used to achieve the required thrust level. Thus, modern turbofan engines are designed to have lower TSFC values as it increases the overall efficiency of the engine and decreases fuel consumption. It is a well-known fact that the TSFC is affected by how much air is let into the turbofan engine. Fan Pressure Ratio (*FPR*) represents the ratio of the fan exit pressure to inlet pressure, and the amount of air being sucked into the engine can be controlled by changing this pressure ratio. As *FPR* is increased in an ideal engine, the nozzle exit Mach number and consequently the jet velocity (V_{jet}) increases. This increase in V_{jet} brings about a decrease in the propulsive efficiency as the two are inversely related. The focus of the work presented in this chapter is to study the performance of the N+3 turbofan engine model while altering the *FPR*.

4.2 Method

For validation of the NPSS model, a MATLAB code from [1] is utilized to study performance of a representative N+3 engine. The flight conditions such as free stream velocity and altitude are set at the start in the code. The necessary propulsive equations discussed in chapter 3 are then used for calculating the performance of different components of the engine. Two different methods are used in the performance calculations: a fixed core method with

constant core mass flow rate and fuel flow rate and thrust convergence method with constant thrust level. In both methods the *BPR* is varied to observe the change in thrust and fuel flow.

The NPSS model contains all the elements and connections that are representative of an N+3 propulsion system. The results of the simulation are defined using viewers that extract data from the system. Moreover, user defined functions, input files, and performance maps of the different engine components are included in the simulation. Both conventional Jet-A fuel and LH_2 fuel are used to evaluate the performance of the engine. It should be noted that there are major design differences between the MATLAB simulation and the NPSS simulation. One of these major design differences is the fact that the NPSS model has multistage compressors and turbines that are defined by detailed maps of the representative N+3 technology. In the MATLAB, the engine is composed of a single stage compressor and turbine that uses simple temperature and pressure calculations with assumed constants. The NPSS model takes predefined dependent variables such as Fnet, Tt4, and OPR and solves for the performance of the engine through the independent variables such as fuel flow, *LPC PR*, and *BPR*. The complete list of the solver dependent and independent variables is given in Fig. 2.

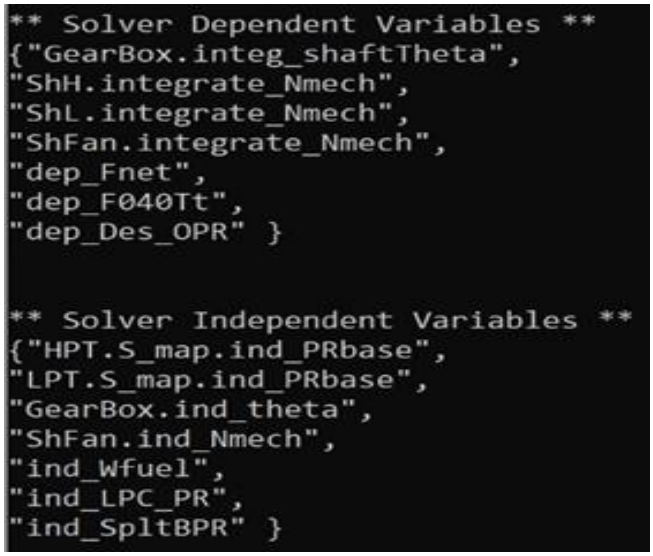

Figure 2: Screenshot of the command prompt window showing NPSS Solver's dependent and independent variables.

Similar flight conditions are used in both the NPSS and MATLAB models. But since the MATLAB engine design is different from the NPSS engine design, the aim of this study is to show the overall trend of the engine performance by varying *BPR* using NPSS and MATLAB and not to dwell on the quantitative comparison. The NPSS simulation is first performed with the Fnet, Tt4, and OPR set to 6126.7 lbf, 3150.0^{o}F, and 55, respectively. A total of seven simulations with *FPR* values of 1.276, 1.3, 1.32, 1.34, 1.36, 1.38, and 1.4 are conducted and the performance data of the engine is recorded at each *FPR* value. As the OPR is fixed in the NPSS engine model, an increase in the *FPR* is mitigated by a decrease in the *BPR*. The performance data obtained from NPSS is then used to replicate the same flight conditions in MATLAB. Thus, the *FPR*, the core mass flow ($\dot{m}_c$), and the *BPR* values of the MATLAB code are all changed to match the values obtained using NPSS. TSFC values corresponding to the each *BPR* are obtained from MATLAB. These values are later used to generate plots that show the relationship between TSFC and *FPR* with *BPR*.

4.3 Results

Figure 3 shows some examples of the viewOut file obtained from NPSS. The viewOut file contains the performance data of the engine. Some important parameters are highlighted in yellow.

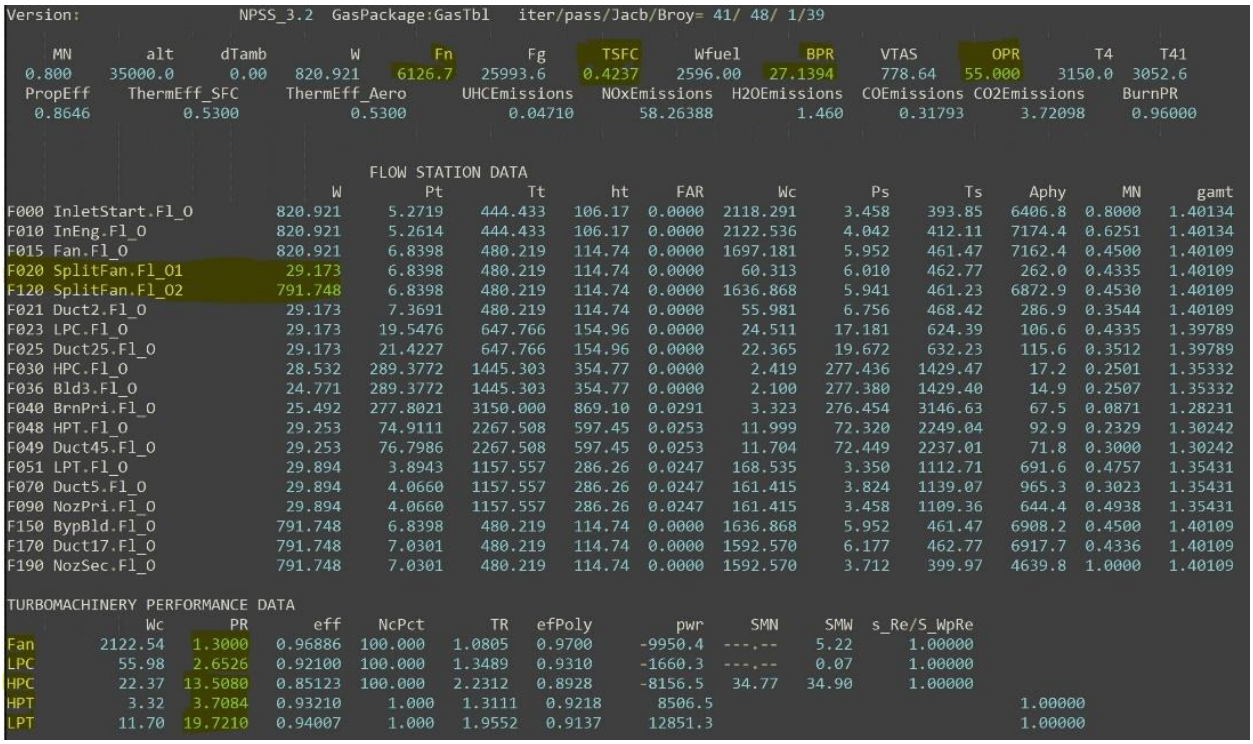

Version: NPSS_3.2 GasPackage:GasTbl iter/pass/Jacb/Broy= 41/ 48/ 1/39

MN	alt	dTamb	W	Fn	Fg	TSFC	Wfuel	BPR	VTAS	OPR	T4	T41
0.800	35000.0	0.00	820.921	6126.7	25993.6	0.4237	2596.00	27.1394	778.64	55.000	3150.0	3052.6

PropEff	ThermEff_SFC	ThermEff_Aero	UHCEmissions	NOxEmissions	H2OEmissions	COEmissions	CO2Emissions	BurnPR
0.8646	0.5300	0.5300	0.04710	58.26388	1.460	0.31793	3.72098	0.96000

FLOW STATION DATA

	W	Pt	Tt	ht	FAR	Wc	Ps	Ts	Aphy	MN	gamt
F000 InletStart.Fl_O	820.921	5.2719	444.433	106.17	0.0000	2118.291	3.458	393.85	6406.8	0.8000	1.40134
F010 InEng.Fl_O	820.921	5.2614	444.433	106.17	0.0000	2122.536	4.042	412.11	7174.4	0.6251	1.40134
F015 Fan.Fl_O	820.921	6.8398	480.219	114.74	0.0000	1697.181	5.952	461.47	7162.4	0.4500	1.40109
F020 SplitFan.Fl_O1	29.173	6.8398	480.219	114.74	0.0000	60.313	6.010	462.77	262.0	0.4335	1.40109
F120 SplitFan.Fl_O2	791.748	6.8398	480.219	114.74	0.0000	1636.868	5.941	461.23	6872.9	0.4530	1.40109
F021 Duct2.Fl_O	29.173	7.3691	480.219	114.74	0.0000	55.981	6.756	468.42	286.9	0.3544	1.40109
F023 LPC.Fl_O	29.173	19.5476	647.766	154.96	0.0000	24.511	17.181	624.39	106.6	0.4335	1.39789
F025 Duct25.Fl_O	29.173	21.4227	647.766	154.96	0.0000	22.365	19.672	632.23	115.6	0.3512	1.39789
F030 HPC.Fl_O	28.532	289.3772	1445.303	354.77	0.0000	2.419	277.436	1429.47	17.2	0.2501	1.35332
F036 Bld3.Fl_O	24.771	289.3772	1445.303	354.77	0.0000	2.100	277.380	1429.40	14.9	0.2507	1.35332
F040 BrnPri.Fl_O	25.492	277.8021	3150.000	869.10	0.0291	3.323	276.454	3146.63	67.5	0.0871	1.28231
F048 HPT.Fl_O	29.253	74.9111	2267.508	597.45	0.0253	11.999	72.320	2249.04	92.9	0.2329	1.30242
F049 Duct45.Fl_O	29.253	76.7986	2267.508	597.45	0.0253	11.704	72.449	2237.01	71.8	0.3000	1.30242
F051 LPT.Fl_O	29.894	3.8943	1157.557	286.26	0.0247	168.535	3.350	1112.71	691.6	0.4757	1.35431
F070 Duct5.Fl_O	29.894	4.0660	1157.557	286.26	0.0247	161.415	3.824	1139.07	965.3	0.3023	1.35431
F090 NozPri.Fl_O	29.894	4.0660	1157.557	286.26	0.0247	161.415	3.458	1109.36	644.4	0.4938	1.35431
F150 BypBld.Fl_O	791.748	6.8398	480.219	114.74	0.0000	1636.868	5.952	461.47	6908.2	0.4500	1.40109
F170 Duct17.Fl_O	791.748	7.0301	480.219	114.74	0.0000	1592.570	6.177	462.77	6917.7	0.4336	1.40109
F190 NozSec.Fl_O	791.748	7.0301	480.219	114.74	0.0000	1592.570	3.712	399.97	4639.8	1.0000	1.40109

TURBOMACHINERY PERFORMANCE DATA

	Wc	PR	eff	NcPct	TR	efPoly	pwr	SMN	SMW	s_Re/S_WpRe		
Fan	2122.54	1.3000	0.96886	100.000	1.0805	0.9700	-9950.4	---.--	5.22	1.00000		
LPC	55.98	2.6526	0.92100	100.000	1.3489	0.9310	-1660.3	---.--	0.07	1.00000		
HPC	22.37	13.5080	0.85123	100.000	2.2312	0.8928	-8156.5	34.77	34.90	1.00000		
HPT	3.32	3.7084	0.93210	1.000	1.3111	0.9218	8506.5				1.00000	
LPT	11.70	19.7210	0.94007	1.000	1.9552	0.9137	12851.3				1.00000	

(a) viewOut file for FPR = 1.3 (Jet-A Fuel)

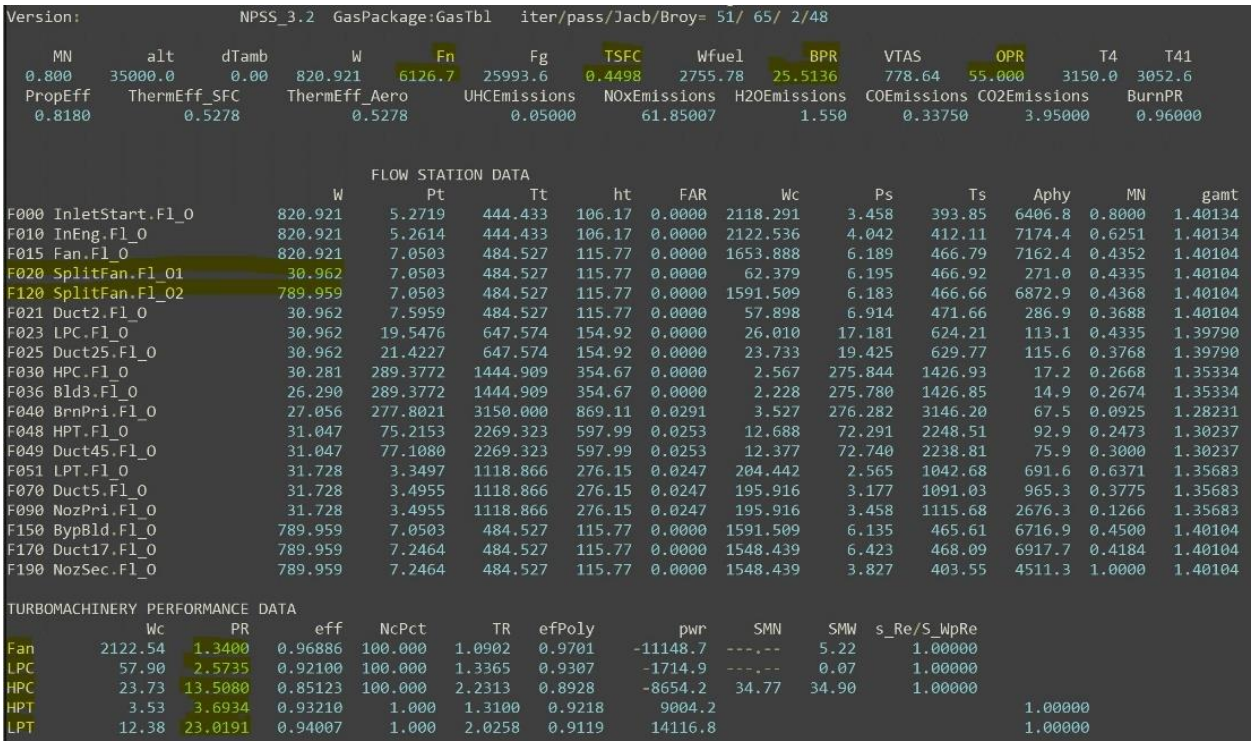

Version: NPSS_3.2 GasPackage:GasTbl iter/pass/Jacb/Broy= 51/ 65/ 2/48

MN	alt	dTamb	W	Fn	Fg	TSFC	Wfuel	BPR	VTAS	OPR	T4	T41
0.800	35000.0	0.00	820.921	6126.7	25993.6	0.4498	2755.78	25.5136	778.64	55.000	3150.0	3052.6

PropEff	ThermEff_SFC	ThermEff_Aero	UHCEmissions	NOxEmissions	H2OEmissions	COEmissions	CO2Emissions	BurnPR
0.8180	0.5278	0.5278	0.05000	61.85007	1.550	0.33750	3.95000	0.96000

FLOW STATION DATA

	W	Pt	Tt	ht	FAR	Wc	Ps	Ts	Aphy	MN	gamt
F000 InletStart.Fl_O	820.921	5.2719	444.433	106.17	0.0000	2118.291	3.458	393.85	6406.8	0.8000	1.40134
F010 InEng.Fl_O	820.921	5.2614	444.433	106.17	0.0000	2122.536	4.042	412.11	7174.4	0.6251	1.40134
F015 Fan.Fl_O	820.921	7.0503	484.527	115.77	0.0000	1653.888	6.189	466.79	7162.4	0.4352	1.40104
F020 SplitFan.Fl_O1	30.962	7.0503	484.527	115.77	0.0000	62.379	6.195	466.92	271.0	0.4335	1.40104
F120 SplitFan.Fl_O2	789.959	7.0503	484.527	115.77	0.0000	1591.509	6.183	466.66	6872.9	0.4368	1.40104
F021 Duct2.Fl_O	30.962	7.5959	484.527	115.77	0.0000	57.898	6.914	471.66	286.9	0.3688	1.40104
F023 LPC.Fl_O	30.962	19.5476	647.574	154.92	0.0000	26.010	17.181	624.21	113.1	0.4335	1.39790
F025 Duct25.Fl_O	30.962	21.4227	647.574	154.92	0.0000	23.733	19.425	629.77	115.6	0.3768	1.39790
F030 HPC.Fl_O	30.281	289.3772	1444.909	354.67	0.0000	2.567	275.844	1426.93	17.2	0.2668	1.35334
F036 Bld3.Fl_O	26.290	289.3772	1444.909	354.67	0.0000	2.228	275.780	1426.85	14.9	0.2674	1.35334
F040 BrnPri.Fl_O	27.056	277.8021	3150.000	869.11	0.0291	3.527	276.282	3146.20	67.5	0.0925	1.28231
F048 HPT.Fl_O	31.047	75.2153	2269.323	597.99	0.0253	12.688	72.291	2248.51	92.9	0.2473	1.30237
F049 Duct45.Fl_O	31.047	77.1080	2269.323	597.99	0.0253	12.377	72.740	2238.81	75.9	0.3000	1.30237
F051 LPT.Fl_O	31.728	3.3497	1118.866	276.15	0.0247	204.442	2.565	1042.68	691.6	0.6371	1.35683
F070 Duct5.Fl_O	31.728	3.4955	1118.866	276.15	0.0247	195.916	3.177	1091.03	965.3	0.3775	1.35683
F090 NozPri.Fl_O	31.728	3.4955	1118.866	276.15	0.0247	195.916	3.458	1115.68	2676.3	0.1266	1.35683
F150 BypBld.Fl_O	789.959	7.0503	484.527	115.77	0.0000	1591.509	6.135	465.61	6716.9	0.4500	1.40104
F170 Duct17.Fl_O	789.959	7.2464	484.527	115.77	0.0000	1548.439	6.423	468.09	6917.7	0.4184	1.40104
F190 NozSec.Fl_O	789.959	7.2464	484.527	115.77	0.0000	1548.439	3.827	403.55	4511.3	1.0000	1.40104

TURBOMACHINERY PERFORMANCE DATA

	Wc	PR	eff	NcPct	TR	efPoly	pwr	SMN	SMW	s_Re/S_WpRe		
Fan	2122.54	1.3400	0.96886	100.000	1.0902	0.9701	-11148.7	---.--	5.22	1.00000		
LPC	57.90	2.5735	0.92100	100.000	1.3365	0.9307	-1714.9	---.--	0.07	1.00000		
HPC	23.73	13.5080	0.85123	100.000	2.2313	0.8928	-8654.2	34.77	34.90	1.00000		
HPT	3.53	3.6934	0.93210	1.000	1.3100	0.9218	9004.2				1.00000	
LPT	12.38	23.0191	0.94007	1.000	2.0258	0.9119	14116.8				1.00000	

b) viewOut file for FPR = 1.34 (Jet A Fuel)

Figure 3: Sample screenshots of the viewOut file obtained from NPPS

As can be seen in Fig. 3, the OPR, Fnet, and HPC PR stay the same even though *FPR* is changing. Moreover, LPC PR, HPT, and LPT changed with *FPR* while their efficiency stayed the same. The other important thing to notice here is that both the core mass flow (represented by SplitFan.F1_01) and the bypass bleed (represented by Splintfan.F1_02) change with *FPR.* However, the two values change with *FPR* in opposite direction, core mass flow in the increasing direction and bypass bleed in the decreasing direction. This leads to an overall decrease in the *BPR* as *BPR* is the ratio of the bypass bleed to the core mass flow.

Figures 4 and 5 show how the TSFC and *BPR* were affected by the change in *FPR* for Jet-A fuel and for LH_2, respectively. As can be seen in the plots, TSFC increased with increasing *FPR* while *BPR* decreased with increasing *FPR* for both fuel types. Higher TSFC value means more fuel is being consumed to achieve the necessary thrust level. Moreover, the observed

increasing trend of the TSFC value is a direct effect of the decrease in the *BPR* value. The *BPR* showed a decreasing trend with an increase in *FPR*. This was because the OPR was kept constant and thus, an increase in *FPR* was mitigated by a decrease in *BPR* to match up the OPR value of 55.

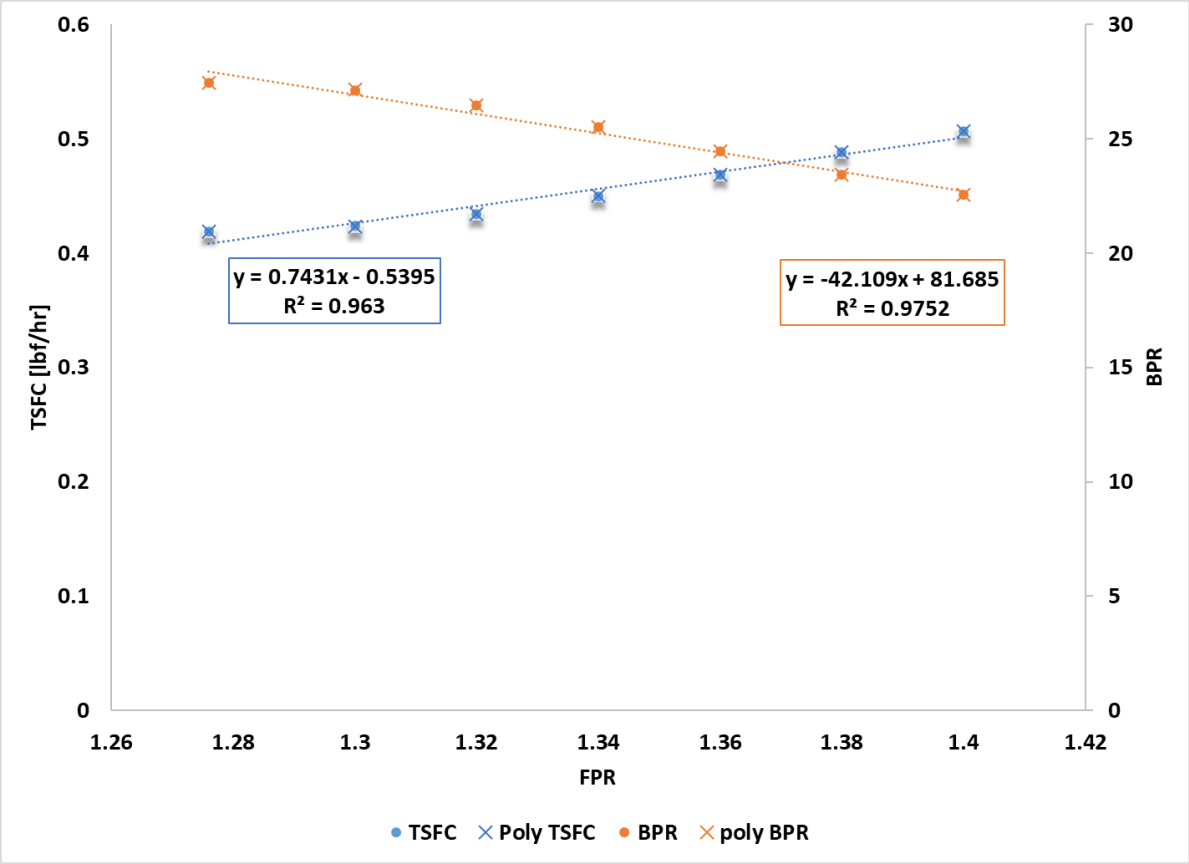

Figure 4: TSFC vs. FPR (primary axis) and BPR vs. FPR (secondary axis) for Jet-A fuel. The linear fit is placed to show the increasing or decreasing trend of the plot. The plots can be fitted well using a polynomial fit of degree 3 (see Appendix A for detail).

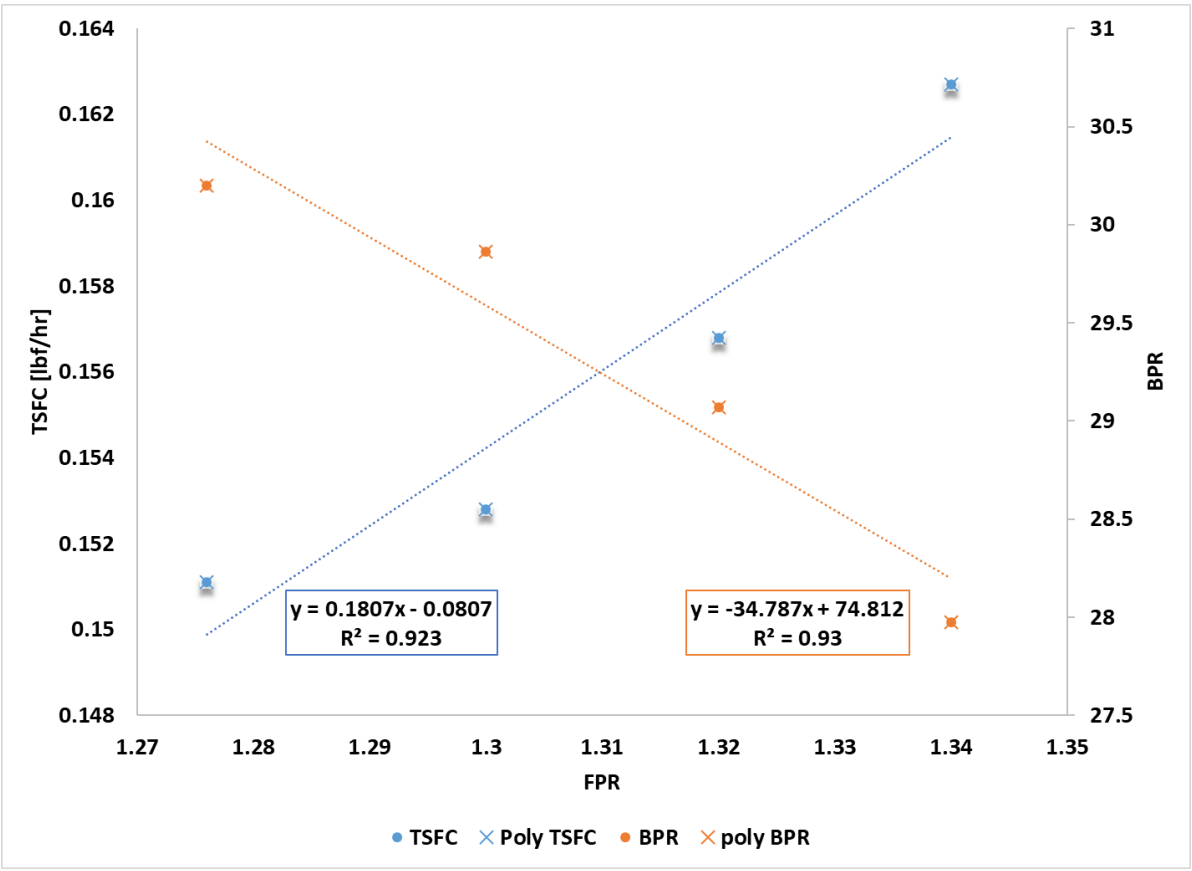

Figure 5: TSFC vs. FPR (primary axis) and BPR vs. FPR (secondary axis) for LH_2 fuel. The linear fit is placed to show the increasing or decreasing trend of the plot. The plots can be fitted well using a polynomial fit of degree 3 (see Appendix A for detail).

Comparing plots in Fig. 4 and Fig. 5, one can see that the TSFC value when using LH_2 fuel is much lower than the TSFC value when using conventional Jet-A fuel. This indicates less amount of fuel (by mass) is needed to reach the required thrust level. This has a direct effect in decreasing both emission and cost of flights as less fuel is being consumed. The above study has been carried out to demonstrate how the engine is being sized in NPSS. The data points from Fig. 4 were then used in the MATLAB code obtained from the appendix of Ref. [1]. (See Appendix A for the modified version of the MATLAB code).

Figure 6 shows the decreasing trend of TSFC with increasing *BPR* of both NPSS and MATLAB simulations run using Jet-A fuel. The plot shows a decrease in TSFC value with an

increase in *BPR*. Even though the flight conditions in NPSS were replicated in MATLAB as much as possible, the difference in the engine designs produces discrepancies. As can be seen in this plot, the NPSS simulation result shows a steep decrease in TSFC with increase in *BPR* compared to the MATLAB simulation results.

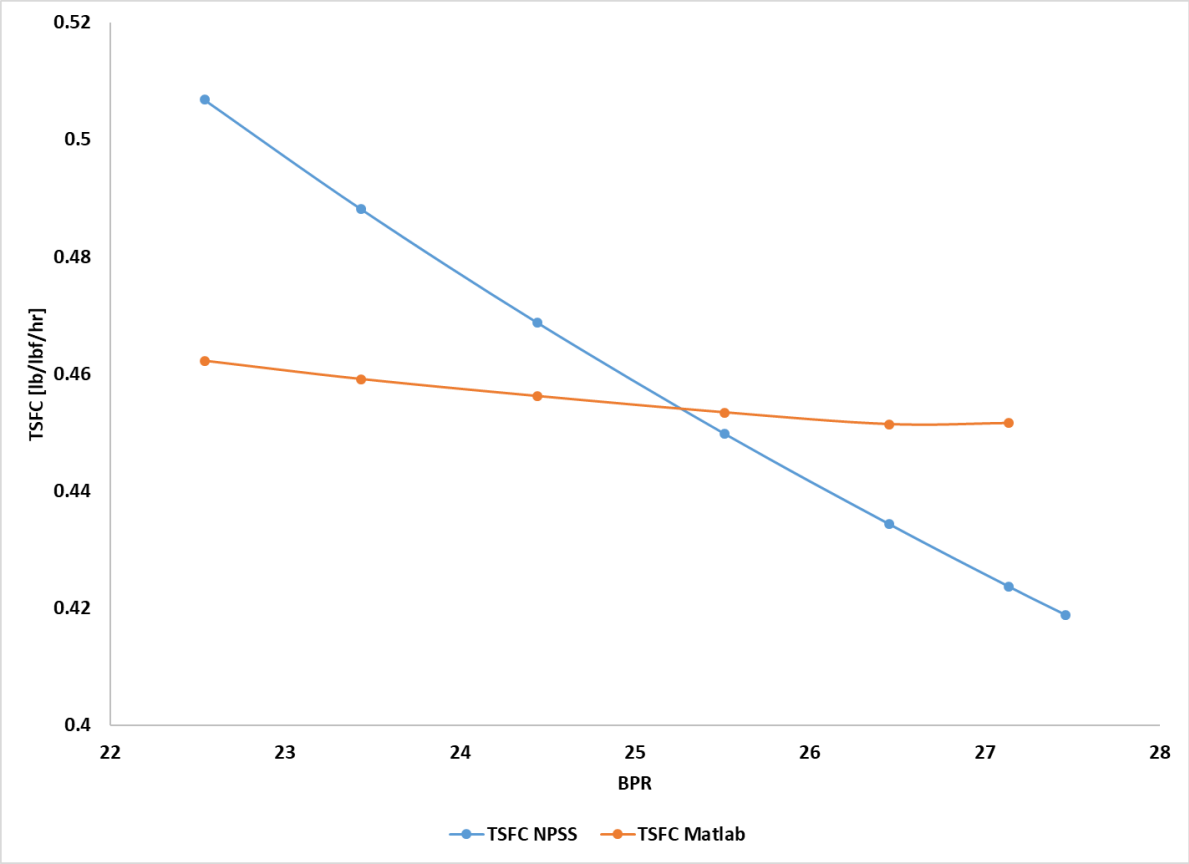

Figure 6: Plot showing the effect of increasing BPR on TSFC using Jet-A as a fuel source.

The steep decrease in TSFC value for NPSS came from the core and bypass bleed design used in the engine model. The NPSS model was set to have a rubber engine, with both the core and the bypass being able to change size each time design iteration is run. An increase in *FPR* brought about an increase in the core mass flow and a decrease in the bypass bleed, thus a decrease in *BPR*. The NPSS model has a double edge sword effect as both the core and the bypass are changing size. In the MATLAB code, however, the core mass flow is kept constant,

thus an increase in *BPR* is achieved through an increase in the bypass bleed only. For this reason, the change in TSFC value is much lower when using the MATLAB simulation compared to when using the NPSS simulation. It is possible to replicate the constant core flow in NPSS and allow only the bypass flow to change, but this would require a completely new set-up for NPSS solver. The fixed core mass flow solver setup is explored in chapter 5.

4.4 Conclusion

Lower TSFC values are desirable in the aviation industry as lower TSFC value would mean less fuel is being used to reach the required thrust. Thus, commercial airlines can cut their fuel cost by mounting an engine with lower TSFC value. However, there is a tradeoff as lower TSFC values are achieved by bigger engines. Hence, both aerodynamic and engine size need to be considered to optimize the fuel consumption of an airplane.

The decrease in TSFC and thus the fuel consumption is beneficial not only financially, but also environmentally as low fuel consumption leads to less greenhouse gas emissions. The lower TSFC values obtained when running LH_2 as opposed to Jet-A give a clear indication that LH_2 is a desirable fuel type both financially and environmentally. Both NPSS and MATLAB simulations achieve the same decreasing trend in TSFC value with an increase in *BPR*. However, the extra capability of NPSS to size a rubber engine and to perform detailed thermodynamics calculations using performance maps gave it an extra edge. This was shown in the steep decrease in the TSFC value compared to the shallower decrease obtained using MATLAB code.

4.5 References

[1] A. Dankanich and D. Peters, “Turbofan Engine Bypass Ratio as a Function of Thrust and Fuel Flow,” *Mech. Eng. Mater. Sci. Dept. Independent Study*, Washington University in St. Louis, Apr. 2017, doi: https://doi.org/10.7936/gps1-kd93.

Chapter 5: Performance Study of N+3 Turbofan Engine Model with Several Types of Fuels Using NPSS

5.1 Introduction

If we keep the *FPR* constant in Eq. 10 introduced in chapter 3, the exit Mach number also becomes constant leading to a constant exit jet velocity. Thus, the propulsive efficiency depends on only one factor that is the free stream velocity V_o. At constant *FPR*, the propulsive efficiency increases with increasingV_o. However, increasing V_o indefinitely is counterproductive since it would decrease the net thrust generated by the engine (see Eq. (8)). The Thrust Specific Fuel Consumption (TSFC) is better suited to study the performance of a turbofan engine in such cases since it incorporates the amount of fuel used for thrust generation. The equation for calculating TSFC is given in Eq. (11):

$$TSFC = \frac{\dot{m}_{fuel}}{T_{net}} \tag{11}$$

where $\dot{m}_{fuel}$ [lb/hr] is the fuel mass flow rate entering the combustor and T_{net} [lbf] is the net thrust generated by the N+3 technology level turbofan engine.

The amount of fuel needed to generate some level of thrust differs based on the type of fuel used. Different fuels have different heating values which are a measure of the amount of energy that can be extracted during combustion. The Higher Heating Value (HHV) indicates the upper limit of the thermal energy produced during combustion while the Lower Heating Value (LHV) indicates the thermal energy produced minus the latent heat of vaporization of water since it

assumes the water produced through combustion is in the vapor form [1]. The useful energy content of fuels is therefore best estimated through LHV. The higher the LHV value, higher is the thermal energy that can be extracted from the fuel.

The aim of this chapter is to study the performance of the N+3 turbofan engine model by altering the *BPR* while keeping the core flow and the *FPR* constant. We also explore alternative fuel sources to conventional Jet-A such as liquid hydrogen (LH_2), liquid natural gas (LNG), and ammonia (NH_3). Their advantages and disadvantages to the performance of the engine and the environment are quantified in this and the subsequent chapter.

5.2 Method

Here again, NPSS is employed to calculate the performance of NASA N+3 geared turbofan engine using different fuels. In keeping with the motivation of this section, the engine was modeled to have constant mass flow through the core and any change in *BPR* is obtained by altering the bypass bleed without changing the core. The solver setup was constructed using dependent and independent variables. The NPSS model utilizes the predefined dependent variables to calculate for the independent variables which are used to analyze the performance of the engine. Table 4 gives a list of the independent and dependent variables used in the solver setup.

Table 4: Dependent and independent variables used for NPSS solver setup

NPSS Solver Variables	
Independent Variables	***Dependent Variables***
Fuel Flow, W_{fuel}	Desired Gross Thrust, F_{gross}
Fan Pressure Ratio, FPR	Desired Burner Temperature, T_{04}

Bypass Ratio, *BPR*	Desired Overall Pressure Ratio, *OPR*

Initial estimations of important design parameters are made by scaling the bypass ratio *BPR* with preliminary calculations while keeping the core flow and *FPR* fixed. The initial estimates (see Appendix B) are used to obtain a desired *BPR* value needed to reach the specified thrust level. The variables that change with *BPR* are included as an input file in NPSS (see Appendix C). Fine tuning of the gross thrust from the initial estimates is necessary to reach at the exact *BPR* level when running the simulation. The NPSS model is simulated with the Tt4, FPR, and OPR set to 3150.0^{o}F, 1.3, and 55, respectively. A total of thirteen simulations with *BPR* values ranging from 1-12 and 20 are conducted and the TSFC of the engine is recorded at each *BPR* value. Once the engine model is validated against the MATLAB code [2] for Jet-A fuel, the same solver setup is employed to study the engine performance using liquid hydrogen (LH_2), liquid natural gas (LNG), and Ammonia (NH_3) as alternative fuels. The results from these simulations can be used to quantify the effect of the fuels' energy content on the TSFC of the gas turbine engine.

5.3 Results

Figure 7 shows the change in TSFC with *BPR* based on results obtained from both MATLAB and NPSS codes. As can be seen from this figure, the results from the two simulations agree within$\pm$8%. Both simulations show a similar decreasing trend for TSFC as *BPR* increases consistent with the well-known relation between the two quantities. However, the TSFC obtained from the NPSS is below that obtained from the MATLAB at lower *BPR* values; it becomes approximately the same around *BPR* = 6 and becomes higher thereafter. NPSS employs an advanced thermochemical calculation model together with detailed engine map data and

turbomachinery configurations and provides more accurate results compared to the simplified calculation model used in MATLAB.

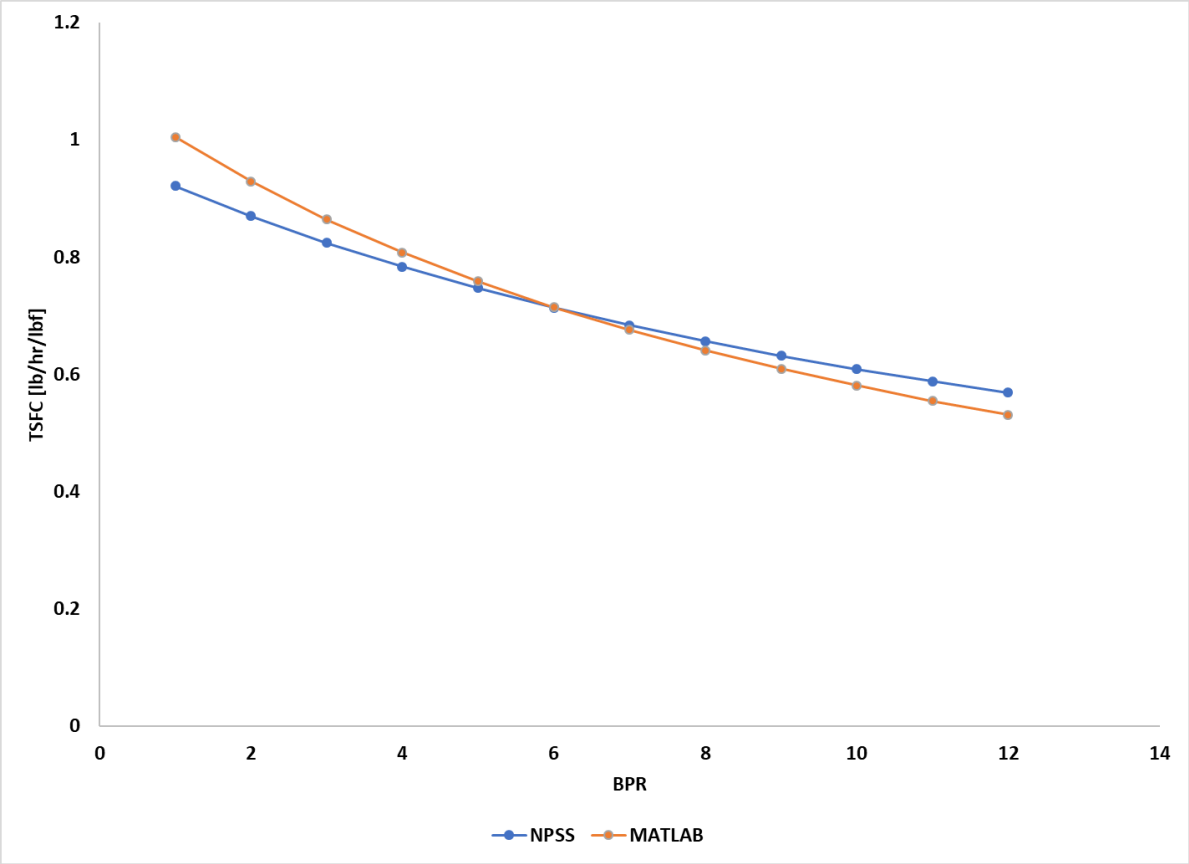

Figure 7: TSFC vs BPR plot comparing the results obtained from MATLAB and NPSS using the fixed core method.

The above result in Fig. 7 demonstrates that the new NPSS solver setup can replicate the fixed core method used in the MATLAB simulation of [2] with good accuracy. The validated NPSS is then used to investigate the performance of alternative fuels (LH_2, LNG, and NH_3) and the results are compared to those of conventional Jet-A fuel. Figure 8 shows a trend of decreasing TSFC with increasing *BPR* for all fuel types. As can be seen from this figure, LH_2 gives the lowest TSFC value while NH_3 gives the highest; Jet-A fuel results are somewhere in the middle with LNG sitting right below it. This trend is consistent with our expectation based on

the heating values of the fuels. LH_2 has the highest LHV (51,621 BTU/lbm) and hence can achieve the required thrust level by burning lower amount of fuel compared to Jet-A which has a LHV of 18550 BTU/lbm. NH_3 has the lowest LHV (7987 BTU/lbm) and would require much more fuel to get to the same thrust level compared to both LH_2 and Jet-A. Compared to the TSFC value using Jet-A as a fuel , using LH_2 decreases TSFC by 62.5% while using NH_3 increases TSFC by 130%.

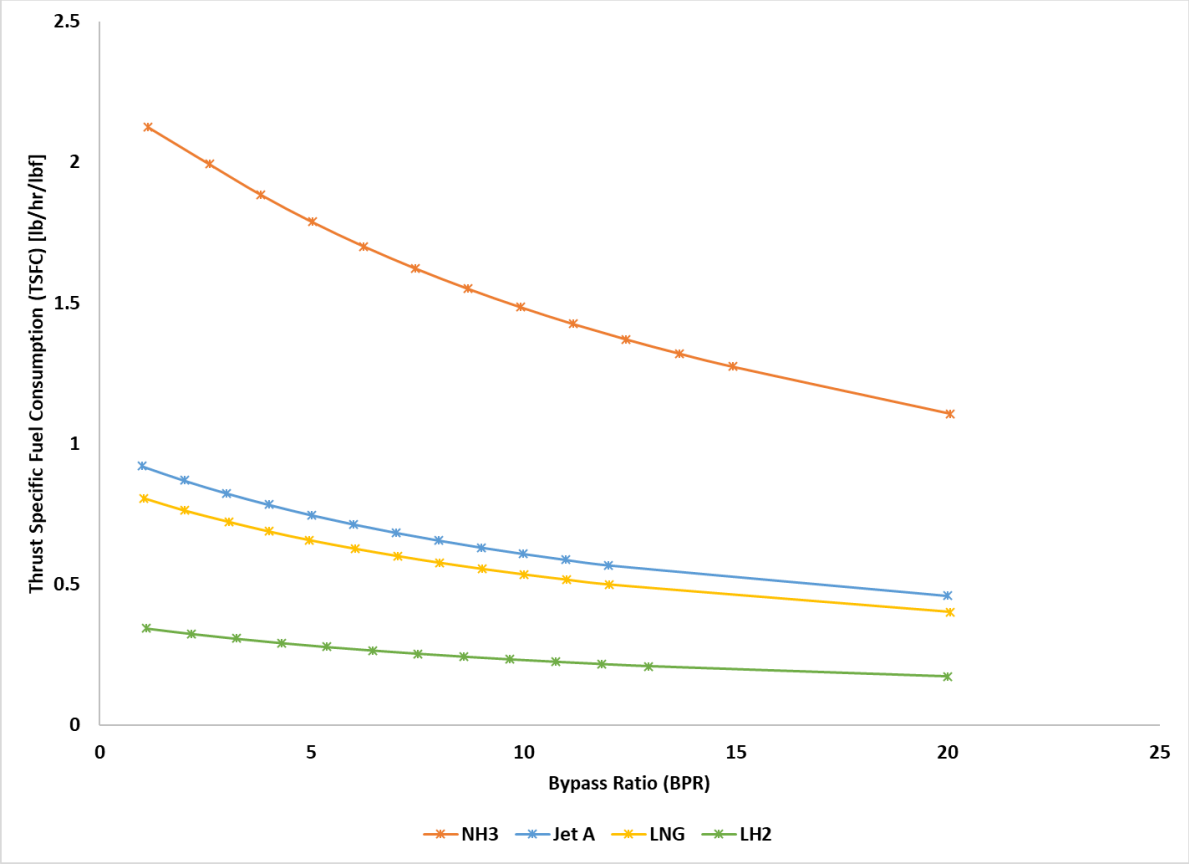

Figure 8: TSFC vs BPR plot comparing the performance of three types of fuels in NPSS: conventional Jet-A, Ammonia (NH3), and Liquid Hydrogen (LH2).

5.4 Conclusion

The new NPSS solver setup for the fixed core method was validated against results obtained from MATLAB. The additional capability of NPSS in performing detailed

thermodynamics calculations using performance maps gives it an extra edge in sizing and studying an engine model. It is concluded that NPSS can be employed with confidence as a preferred engine performance study tool for research, development, and design of new propulsion systems.

From the study of *BPR* sensitivity on TSFC, it was shown that there is a direct relationship between TSFC and LHV of a fuel. The higher the LHV value of a fuel, the lower is TSFC value. This implies that less fuel is required (by mass) if for example conventional Jet-A fuel is replaced by LH_2. The volume needed to store LH_2, however would be much higher due to its low density. In addition, having LH_2 on board would require a lot more energy since it needs to be kept in a cryogenic tank due to its extremely low boiling temperature [3]. Due to its high volatility, care must be taken during handling. Nonetheless, the environmental benefits of using LH_2, with zero carbon and low NOx emissions, make it a great candidate as an alternative fuel source for sustainable and environmentally friendly aviation. With future advancements in technology and research findings, improved LH_2 delivery and storage infrastructures can be developed to use it as a main source of fuel in aviation. Even though the low LHV of NH_3 makes it less desirable for usage as a fuel source by itself, its environmental benefit and abundance make it a worthwhile alternative fuel source to study.

5.5 References

[1] "Glossary - U.S. Energy Information Administration (EIA)." https://www.eia.gov/tools/glossary/index.php

[2] A. Dankanich and D. Peters, "Turbofan Engine Bypass Ratio as a Function of Thrust and Fuel Flow," *Mech. Eng. Mater. Sci. Indep. Study*, Washington University in St. Louis, Apr. 2017, doi: https://doi.org/10.7936/gps1-kd93.

[3] “Hydrogen as Aviation Fuel: A Comparison with Hydrocarbon Fuels - ScienceDirect.” https://www.sciencedirect.com/science/article/pii/S0360319997000086?via%3Dihub

Chapter 6: Emission studies of N+3 and N+4 Technology Level Propulsion Systems with Alternative Fuels

6.1 Introduction

This section outlines the development of a method for estimating emissions within the NPSS framework by utilizing the performance parameters of the N+3 and N+4 geared turbofan engine models published by NASA [1, 2]. Validation of this method is demonstrated by comparing the emissions indexes of Jet-A and LH_2 fuels with published data. Furthermore, the NPSS model is utilized to analyze the emissions and performance of LNG, NH_3 cracking and thermal decomposition of Ammonia-Borane (AB). A detailed description of the emissions calculation and performance comparison between Jet-A and other fuels (LNG, LH_2, NH_3, and AB) is discussed. However, it should be noted that these results are intended to demonstrate trends when comparing alternative fuels and require additional experimental data to conduct a more accurate analyses.

6.2 Methods

NPSS allows for importing emissions indexes into the software's emissions element as a post-processing function. However, accurately predicting the products of combustion for non-metals is challenging due to their dependence on temperature, pressure, fuel-to-air ratio, ignition timing, and thermal dilution, among others. Therefore, it is crucial to have experimental data with conditions that match the modeled scenario to generate accurate indices for use in NPSS models. Although NPSS can be connected to high fidelity computational fluid dynamics tools, it does not perform specific gas dynamics modeling. To enhance NPSS's capability in providing

accurate data for engine performance, an emissions estimation function is developed and validated against published emissions indices. Tables 5 and 6 display the emissions indices obtained from prior investigations on Jet-A and LH_2 combustion in a turbofan engine utilizing NPSS [3]. These indices serve as validation benchmarks until a more extensive experimental data becomes accessible. Assuming the power setting at cruise to be 90% for N+3 and 80% for N+4, the emissions indices of both engines can be determined through linear interpolation.

Table 5: Emissions Indexes for Jet-A.

Emission Indexes						
JetA	Power Setting	NOx [g/kg fuel]	UHC [g/kg fuel-1]	CO [g/kg fuel]	CO2 [g/kg]	H20 [g/kg]
Take-off	100	49.48	0.04	0.27	3.16	1.24
Climb	85	21.03	0.04	0.23	3.16	1.24
Approach	30	9.27	0.05	2.21	3.16	1.24
Idle	7	4.72	0.25	20.3	3.16	1.24

Table 6: Emissions Indexes for Liquid Hydrogen (LH2).

Emission Indexes						
LH2	Power Setting	NOx [g/kg fuel]	UHC [g/kg fuel-1]	CO [g/kg fuel]	CO2 [g/kg]	H20 [g/kg]
Take-off	100	37.6048	0	0	0	8.94
Climb	85	15.9828	0	0	0	8.94
Approach	30	7.0452	0	0	0	8.94
Idle	7	3.5872	0	0	0	8.94

The stoichiometric combustion reactions in chapter 2 are inadequate to accurately estimate emissions for lean mixtures. This is because combustion reactions involve a series of single-step reactions with short-lived species and high reaction rates that cannot be represented by a simple balanced stoichiometric chemical equation [4]. Therefore, this study considers the dominant reaction equations based on the operating environmental conditions. The potential

reactions that may occur during LH_2 and NH_3 combustion are presented in Tables 7 and 8, respectively.

Table 7: Elementary reaction steps for combustion of Liquid Hydrogen (LH_2) [5].

LH_2 Combustion in Air Reaction Equations
$H + O_2 \Leftrightarrow O + OH$
$O + H_2 \Leftrightarrow H + OH$
$OH + H_2 \Leftrightarrow H + H_2O$
$O + H_2O \Leftrightarrow OH + OH$
$H_2 + M \Leftrightarrow H + H + M$ $H_2 + Ar$
$O + O + M \Leftrightarrow H_2O + Ar$ $O + O + Ar \Leftrightarrow H_2O + Ar$
$O + H_2 \Leftrightarrow OH + H$
$O + OH + M \Leftrightarrow H_2O + M$ $H + OH + Ar \Leftrightarrow H_2O + Ar$
$H + O_2 + M \Leftrightarrow HO_2 + M$ $H + O_2 + Ar \Leftrightarrow HO_2 + Ar$ $H + O_2 \Leftrightarrow HO_2$
$HO_2 + HO_2 \Leftrightarrow H_2O_2 + O_2$
$HO_2 + H \Leftrightarrow H_2 + O_2$
$HO_2 + O \Leftrightarrow O_2$
$HO_2 + OH \Leftrightarrow H_2O + O_2$
$HO_2 + HO_2 \Leftrightarrow H_2O_2 + O_2$
$H_2O_2 + M \Leftrightarrow OH + OH + M$ $H_2O_2 + Ar \Leftrightarrow OH + OH + Ar$ $H_2O_2 \Leftrightarrow OH + OH$
$H_2O_2 + H \Leftrightarrow H_2O + OH$
$H_2O_2 + H \Leftrightarrow H_2 + HO_2$
$H_2O_2 + O \Leftrightarrow OH + HO_2$

$H_2O_2 + OH \Leftrightarrow H_2O + HO_2$

Table 8: Elementary reaction steps for combustion of Ammonia (NH_3) [4].

NH_3 Combustion in Air Reaction Equations
$NH_3 + OH \Leftrightarrow H_2O + NH_2$
$NH_2 + NO \Leftrightarrow H_2O + N_2$
$NH_2 + OH \Leftrightarrow H_2O + NH$
$NNH + O_2 \Leftrightarrow HO_2 + N_2$
$H + O_2 \Leftrightarrow O + OH$
$H + NO + M \Leftrightarrow HNO + M$
$2OH \Leftrightarrow H_2O + O$

The Chemical Equilibrium Applications (CEA) thermo-package was selected to conduct the thermodynamic analysis. By using results from the LH_2 combustion, estimations for hydrogen carrier options like catalytic NH_3 cracking and the thermal decomposition of AB can be easily calculated. Under NPSS's CEA thermo-package, the Gibbs free energy is calculated from a balanced combustion reaction and information about the temperature, pressure, and transferred energy is passed on to the next cycle [6]. The Gibbs free energy equation shown in Eq. 12 gives the energy produced with each reaction step. The built-in CEA thermo-package in NPSS calculates the energy extracted from a combustion reaction using this equation.

$$\Delta G = \Delta H - T\Delta S \tag{12}$$

Here, ΔG [kJ] represents the change in Gibbs free energy, ΔH [kJ] is the enthalpy extracted from combustion of the fuel, ΔS [kJ/K] is the change in entropy of the system, and T [K] is the absolute temperature.

Preliminary research conducted in chapter 5 with Jet-A, LH_2, LNG, and NH_3 indicated varying performance characteristics. Moreover, previous published studies have demonstrated that having higher LHV fuels can assist in expanding the compressor surge margin [7]. Thus, accurate performance evaluation has great importance in determining the right fuel type for a specific flight condition. To accurately represent the progression of the combustion, a detailed analysis on the rate of combustion reaction is needed. The addition of reaction rate in the simulation would help to predict emissions with better accuracy. However, this can only be achieved with detailed combustion modeling for which NPSS is not well suited. NPSS works most efficiently with tabulated emissions indexes such as Table 5 and 6. For NH_3 cracking and thermal decomposition of AB, it is assumed that no Nitrogen or Boron will enter the combustion chamber and thus, their emissions are estimated to be similar to liquid hydrogen emissions.

6.3 Results

Tables 9-11 show the performance and emissions of N+3 technology level engine when operated using alternative fuels as compared to Jet-A. While Jet-A, LH_2, and NH_3 are run using the data in the CEA thermo-package, NH_3 cracking and the thermal decomposition of AB are run as the NH_3 and LH_2 fuels, respectively with updated LHVs. LNG is run using CEA thermo-package by assuming that it is fully composed of CH_4 but with an updated LHV that corresponds to LNG. Although not accurate, this assumption is valid since LNG is mainly composed of CH_4 (usually 85-95%) [8]. For catalytic cracking of NH_3, the assumption is 3 mole of H_2 is produced per 2 mole of NH_3 [9]. The byproducts of NH_3 cracking, mainly Nitrogen and its derivatives, are assumed to be expelled into the ambient air through the nozzle. For thermal decomposition of AB, 2 moles of H_2 are produced per 1 mole of AB. Since the combustion of AB produces

crystalline products at the operating burner temperature (T4), the thermal decomposition of AB must happen in a separate unit before fuel injection.

Table 9: Performance and emissions comparison using Jet-A, LH_2, and NH_3 for N+ 3 engine model

Cruise N+3	Jet A	LH2	% Diff From Jet A	NH3	% Diff from Jet A
Altitude [ft.]	35000	35000	**0.00%**	35000	**0.00%**
Mach	0.8	0.8	**0.00%**	0.8	**0.00%**
dTamb	0	0	**#DIV/0!**	0	**0.00%**
Inlet W [lbm/s]	795.64	795.64	**0.00%**	795.64	**0.00%**
Thrust [lbf]	5465.8	5465.8	**0.00%**	5465.8	**0.00%**
SFC	0.4694	0.1692	**-63.95%**	1.0253	**118.43%**
Fuel W [lbm/hr]	2565.48	924.84	**-63.95%**	5604.34	**118.45%**
OPR	51.462	51.462	**0.00%**	51.462	**0.00%**
Fan PR	1.276	1.276	**0.00%**	1.276	**0.00%**
BPR	24.794	27.141	**9.47%**	31.038	**25.18%**
T4 [R]	3035.1	3035.1	**0.00%**	3035.1	**0.00%**
T41 [R]	2941.4	2941.4	**0.00%**	2941.4	**0.00%**
UHCs [kg/hr]	0.05	0.00	**-100.00%**	0.00	**-100.00%**
CO [kg/hr.]	0.28	0.00	**-100.00%**	0.00	**-100.00%**
CO_2 [kg/hr.]	3.68	0.00	**-100.00%**	0.00	**-100.00%**
NOx [kg/hr.]	35.50	9.73	**-72.60%**	Much Higher	**+ UNDET**
H_2O [kg/hr.]	1.44	3.75	**159.90%**	Much Higher	**+ UNDET**

The simulation in NPSS does not account for the extra energy needed to thermally decompose AB and thus the specific fuel consumption (SFC) value would be higher than what is given in Table 10. Moreover, only about 13% by mass of AB is turned into hydrogen and thus, the remaining 87% of AB must be stored or sustainably jettisoned.

Table 10: Performance and emissions comparison using Jet-A, NH_3 cracking, and thermal decomposition of AB for N+3 engine model.

Cruise N+3	Jet A	NH3 Cracking	% Diff From Jet A	Thermal Decomp AB	% Diff from Jet A
Altitude [ft.]	35000	35000	**0.00%**	35000	**0.00%**
Mach	0.8	0.8	**0.00%**	0.8	**0.00%**
dTamb	0	0	**0.00%**	0	**0.00%**
Inlet W [lbm./s]	795.64	795.64	**0.00%**	795.64	**0.00%**
Thrust [lbf.]	5465.8	5465.8	**0.00%**	5465.8	**0.00%**
SFC	0.4694	0.9714	**106.95%**	1.0253	**118.43%**
Fuel W [lbm./hr.]	2565.48	5309.5	**106.96%**	5604.34	**118.45%**
OPR	51.462	51.462	**0.00%**	51.462	**0.00%**
Fan PR	1.276	1.276	**0.00%**	1.276	**0.00%**
BPR	24.794	27.695	**11.70%**	31.038	**25.18%**
T4 [R]	3035.1	3035.1	**0.00%**	3035.1	**0.00%**
T41 [R]	2941.4	2941.4	**0.00%**	2941.4	**0.00%**
UHCs [kg/hr.]	0.05	0.00	**-100.00%**	0.00	**-100.00%**
CO [kg/hr.]	0.28	0.00	**-100.00%**	0.00	**-100.00%**
CO_2 [kg/hr.]	3.68	0.00	**-100.00%**	0.00	**-100.00%**
NOx [kg/hr.]	35.50	55.85	**57.29%**	58.95	**66.02%**
H_2O [kg/hr.]	1.44	21.53	**1392.11%**	8.94	**519.56%**

Table 11: Performance and emissions comparison using Jet-A and LNG for N+3 engine model

Cruise N+3	Model w/ Jet A		Model w/ LNG	% Diff From Jet A
Altitude [ft]	35000		35000	**0.00%**
Mach	0.8		0.8	**0.00%**
dTamb	0		0	**#DIV/0!**
Inlet W [lbm/s]	795.64		795.64	**0.00%**
Thrust [lbf]	5465.8		5465.8	**0.00%**
SFC	0.4694		0.4163	**-11.31%**
Fuel W [lbm/hr]	2565.48		2275.37	**-11.31%**
OPR	51.462		51.462	**0.00%**
Fan PR	1.276		1.276	**0.00%**
T4 [R]	3035.1		3035.1	**0.00%**
T41 [R]	2941.4		2941.4	**0.00%**
UHCs [kg/hr]	0.05		UNKWN	**UNDET**
CO [kg/hr]	0.28		UNKWN	**UNDET**
CO2 [kg/hr]	3.68		2.57	**-30.00%**
NOx [kg/hr]	35.50		7.10	**-80.00%**
H2O [kg/hr]	1.44		1.44	**0.00%**

Tables 12-14 present the NPSS simulation results for the N+4 technology level engine model. As discussed in chapter 3, the N+4 engine has a smaller fan diameter, lower thrust, and lower bypass ratio as compared to the N+3 engine (see Table 3). Thus, larger SFC values are recorded for N+4 engines. Apart from this, no major difference was observed on the performance of alternative fuels between the N+3 and N+4 engine models. One can see the difference in emissions is merely due to the difference in the thrust level of the two engines and hence the fuel burn rate.

Table 12: Performance and emissions comparison using Jet-A, LH_2, and NH_3 for N+4 engine model

Cruise N+4	Jet A	LH2	% Diff From Jet A	NH3	% Diff from Jet A
Altitude [ft.]	38000	38000	**0.00%**	38000	**0.00%**
Mach	0.7	0.7	**0.00%**	0.7	**0.00%**
dTamb	0	0	**0.00%**	0	**0.00%**
Inlet W [lbm/s]	427.68	427.68	**0.00%**	427.68	**0.00%**
Thrust [lbf]	3145	3145	**0.00%**	3145	**0.00%**
SFC	0.5148	0.1853	**-64.01%**	1.1228	**118.10%**
Fuel W [lbm/hr]	1618.92	582.79	**-64.00%**	3531.3	**118.13%**
OPR	51.462	51.462	**0.00%**	51.462	**0.00%**
Fan PR	1.276	1.276	**0.00%**	1.276	**0.00%**
BPR	21.612	23.669	**9.52%**	27.088	**25.34%**
T4 [R]	3035.1	3035.1	**0.00%**	3035.1	**0.00%**
T41 [R]	2941.4	2941.4	**0.00%**	2941.4	**0.00%**
UHCs [kg/hr.]	0.03	0.00	**-100.00%**	0.00	**-100.00%**
CO [kg/hr.]	0.18	0.00	**-100.00%**	0.00	**-100.00%**
CO_2 [kg/hr.]	2.32	0.00	**-100.00%**	0.00	**-100.00%**
NOx [kg/hr.]	22.40	4.01	**-82.10%**	Much Higher	**+ UNDET**
H_2O [kg/hr.]	0.91	2.36	**159.54%**	Much Higher	**+ UNDET**

Table 13: Performance and emissions comparison using Jet-A, NH_3 cracking, and thermal decomposition of AB for N+4 engine model.

Cruise N+4	Jet A	NH3 Cracking	% Diff From Jet A	Thermal Decomp AB	% Diff from Jet A
Altitude [ft.]	38000	38000	**0.00%**	38000	**0.00%**
Mach	0.7	0.7	**0.00%**	0.7	**0.00%**
dTamb	0	0	**0.00%**	0	**0.00%**
Inlet W [lbm./s]	427.68	795.64	**86.04%**	795.64	**86.04%**
Thrust [lbf.]	3145	5465.8	**73.79%**	5465.8	**73.79%**
SFC	0.5148	0.1692	**-67.13%**	1.0253	**99.16%**
Fuel W [lbm./hr.]	1618.92	924.84	**-42.87%**	5604.34	**246.18%**
OPR	51.462	51.462	**0.00%**	51.462	**0.00%**
Fan PR	1.276	1.276	**0.00%**	1.276	**0.00%**
BPR	21.612	27.141	**25.58%**	31.038	**43.61%**
T4 [R]	3035.1	3035.1	**0.00%**	3035.1	**0.00%**
T41 [R]	2941.4	2941.4	**0.00%**	2941.4	**0.00%**
UHCs [kg/hr.]	0.03	0.00	**-100.00%**	0.00	**-100.00%**
CO [kg/hr.]	0.30	0.00	**-100.00%**	0.00	**-100.00%**
CO_2 [kg/hr.]	2.32	0.00	**-100.00%**	0.00	**-100.00%**
NOx [kg/hr.]	14.66	6.36	**-56.58%**	38.57	**163.10%**
H_2O [kg/hr.]	0.91	3.75	**311.87%**	22.73	**2395.83%**

Table 14: Performance and emissions comparison using Jet-A and LNG for N+4 engine model

Cruise N+4	Model w/ Jet A		Model w/ LNG	% Diff From Jet A
Altitude [ft]	38000		38000	**0.00%**
Mach	0.7		0.7	**0.00%**
dTamb	0		0	**0.00%**
Inlet W [lbm/s]	427.68		427.68	**0.00%**
Thrust [lbf]	3145		3145	**0.00%**
SFC	0.5148		0.4565	**-11.32%**
Fuel W [lbm/hr]	1618.92		1435.71	**-11.32%**
OPR	51.462		51.462	**0.00%**
Fan PR	1.276		1.276	**0.00%**
T4 [R]	3035.1		3035.1	**0.00%**
T41 [R]	2941.4		2941.4	**0.00%**
UHCs [kg/hr]	0.03		UNKWN	**UNDET**
CO [kg/hr]	0.18		UNKWN	**UNDET**
CO2 [kg/hr]	2.32		1.62	**-30.01%**
NOx [kg/hr]	22.40		4.48	**-80.00%**
H2O [kg/hr]	0.91		0.91	**0.00%**

6.4 Conclusion

Here, NPSS was employed to study performance and emissions of N+3 and N+4 engines running on Jet-A, LNG, LH_2, NH_3, and Ammonia – Borane (AB). General cruise cycle performance and emissions data are presented to aid in further research efforts for aircraft and propulsion system designs that take emissions into account. The study showed that LH_2 is by far the cleanest fuel source with no carbon emission and minimal NOx emissions. The emissions from the hydrogen carriers (NH_3 cracking and thermal decomposition of AB) are assumed to be the same as LH_2 emissions, considering that only H_2 is used to generate the necessary thrust.

Emissions from the unused byproducts of the hydrogen carriers would either add a weight penalty if kept aboard the aircraft or would contribute to pollution if they are jettisoned to the environment. Since the applicability of liquid hydrogen is limited by the difficulty in transportation and storage, the best alternative fuel source that can be used currently is LNG. The already existing infrastructure supports the transportation of LNG and only minimal modification of propulsion systems would make it possible to use LNG. The main drawback of LNG is the high ignition temperature needed to get the combustion started.

Lastly, it should be noted that although this study utilizes tabulated indexes to estimate emissions, it is not an accurate representation of the actual emissions that involve complex multiple single-step combustion reactions. For future studies, a more accurate emissions calculation that uses burner air flow entry conditions and fuel to air ratio values should be used to estimate the emissions directly from the stoichiometric combustion reaction.

6.5 References

[1] S. M. Jones, W. J. Haller, and M. T.-H. Tong, "An N+3 Technology Level Reference Propulsion System," E-19373, May 2017. [Online]. Available: https://ntrs.nasa.gov/citations/20170005426

[2] M. K. Bradley and C. K. Droney, "Subsonic Ultra Green Aircraft Research Phase II: N+4 Advanced Concept Development," NF1676L-14434, May 2012. [Online]. Available: https://ntrs.nasa.gov/citations/20120009038

[3] R. E. Carter and R. K. Agarwal, "Development of a Liquid Hydrogen Combustion High Bypass Geared Turbofan Model in NPSS," AIAA Paper 2022-3431, in AIAA Aviation 2022 Forum, Chicago. IL, 29 June - 1 July 2022, doi: 10.2514/6.2022-3431.

[4] Alison Tomlin, "Combustion Chemistry," Princeton-Combustion Institute, 2022. [Online]. Available: https://cefrc.princeton.edu/sites/g/files/toruqf1071/files/documents/Lecture%20Notes%20-%20Tomlin.pdf

[5] T. J. Kim, R. A. Yetter, and F. L. Dryer, “New Results on Moist CO Oxidation: High Pressure, High Temperature Experiments and Comprehensive Kinetic Modeling,” Symp. Int. Combust., Vol. 25, No. 1, pp. 759–766, Jan. 1994, doi: 10.1016/S0082-0784(06)80708-3.

[6] “NPSS Thermodynamics Guide V.3.2.” Southwest Research Institute, San Antonio, TX.

[7] C. A. Palmer, M. R. Erbes, and P. A. Pechtl, “Gatecycle Performance Analysis of the LM 2500 Gas Turbine Utilizing Low Heating Value Fuels." ASME, Gas Turbine Conference, New York, Vol. 8, 1993, pp. 69-76.

[8] “Liquified Natural Gas: Understanding te Basic Facts.” U.S. Department of Energy Office of Fossil Energy, Aug. 2005. [Online]. Available: https://www.energy.gov/sites/prod/files/2013/04/f0/LNG_primerupd.pdf

[9] I. Lucentini, X. Garcia, X. Vendrell, and J. Llorca, “Review of the Decomposition of Ammonia to Generate Hydrogen,” Ind. Eng. Chem. Res., Vol. 60, No. 51, 2021, pp. 18560–18611, doi: 10.1021/acs.iecr.1c00843.

Chapter 7: Summary

This thesis explores future propulsion systems for commercial aircrafts that are currently under development namely the N+3 and N+4 technology level engines. These engines are suitable as propulsion system for an advanced single-aisle aircrafts. Their performance and associated emissions are evaluated. In addition, possible alternative fuel sources are explored with the goal of minimizing emissions while supplying the necessary thrust. The main tool used for performance and emissions evaluation was NPSS.

The validation of the NPSS code was done by comparing its results with results obtained from purely equation based MATLAB code. The usage of compressor maps and detailed thermodynamic tables in NPSS, as opposed to the user supplied limited inputs in MATLAB, brought about slight differences in the results between the two. However, the overall trend and accuracy of the NPSS code was effectively validated.

The results from bypass ratio (*BPR*) sensitivity study showed that there is a significant improvement in thrust specific fuel consumption (TSFC) with increasing *BPR*, giving a step reduction in TSFC at low *BPR* levels which ultimately stabilizes to a smaller reduction of TSFC at higher *BPR* levels. Since increasing the *BPR* ultimately increase the engine size introducing the undesirable consequence of increasing drag, it is crucial to find the optimal *BPR* level for the engine operation. The *BPR* sensitivity study presented in this thesis can be used as a starting point in sizing an engine during design process.

The performance and emissions study of the N+3 and N+4 engines showed that using liquid hydrogen (LH_2) instead of Jet-A gives the lowers fuel consumption rate showing a reduction of 64%. Liquefied natural gas (LNG) follows liquid hydrogen with a 11% fuel

consumption reduction while using ammonia (NH_3) and ammonia-borane (AB) increases the fuel consumption rate by more than 100%. The rate of fuel consumption directly dictates the amount of emissions, thus fuels that lower SFC are the right choice to reduce emissions. Looking at the emissions associated with each fuel, LH_2 is by far the cleanest energy source with no associated carbon emissions and a 72% reduction in NOx emissions as compared to Jet-A. LNG reduces CO_2 and NOx emissions by about 30% and 80% respectively. Although there is no carbon emission associated with NH_3 and AB, they have much higher NOx emissions compared to Jet-A. Although the emissions study presented in this thesis uses indexes, having robust models that can accurately predict emissions associated with alternative fuels are essential for the acceleration of technology development and implementation. In the absence of experimental data, the results presented in this work can be used as a reference for future attempts to enhance the accuracy of emissions estimation model.

Appendix A: MATLAB Code

The MATLAB code shown below is used to validate the NPSS simulation results.

```
%%%%%%%%%%% MEMS 500 Independent Study
%%%%%%%%%%%%%%%%%%%%%%%%%%%%%%%%%%%
%%%%%%%%%%% Andrew Dankanich %%%%% Fall 2016 / Spring
2017%%%%%%%%%%%%%%%%
%%%%%%%%%%% Modified for use by Abel Solomon & Richard Carter %% Fall
2021
clear;
close all;
clc;
%%%%% Flight Conditions and Free Stream
Constants%%%%%%%%%%%%%%%%%%%%%%%%%%
M0 = 0.8; % Free Stream Mach Number 0.88 for this code and 0.8 for NPSS
gc = 32.2 ; %constant lbf to lbm
R = 287; %kJ/kg universal gas constant
g = 1.4; % Gamma for Air
alt = 35000; %Feet, This is not directly used, but coincides with T0
and P0
rec = 0.995; % Inlet Recovery
% 0.995 for NPSS and 0.96 for this code
T0 = 219; % K Free stream temperature at 35k
% this code has 233: 219 for npss
P0 = 24; % kPa Free stream pressure at 35k
% 24 for NPSS 15 for matlab
a0 = sqrt(g*R*T0); % m/s
Pt0 = P0 * (1+((g-1)/2)*M0^2)^(g/(g-1)); % lbf/ft^2
Tt0 = T0 * (1+((g-1)/2)*M0^2); % R
mft0 = sqrt(g)*M0*(1+((g-1)/2)*M0^2)^-((g+1)/(2*(g-1)));
u0 = M0*sqrt(g*R*T0); %Free Stream Velocity
den0 = P0/(R*T0); %Free Stream Density
%%%%%%%%%%%%%%%%%%%%%%%%%%%

bpr = [27, 27.5, 27.9744, 28.5, 29.0687, 29.5, 29.8607, 30.1987,
30.5,...
    31, 31.5, 32]; %Various Bypass Ratios
% FOR EVERY ITTERATION CHANGE THIS TO MATCH UP TO THE BPR RANGE
% CORESPONDING TO THE FPR USED
sz = length(bpr);
n = 0;

%%%%%%%%%%%%%%%%%%%%%%%%%%
for j = bpr
BPR = j;
```

```
mdotc = 12.85; % UPDATE FOR EVERY ITTERATION USING NPSS DATA CHANGE
FROM
% lbm/s to kg/s
% kg/s CORE AIRFLOW ONLY. This remains constant for all BPR
% and through "guess and check" yields around 30,000lbf for the
turbojet
% configuration (BPR = 0) 162.5 kg/s for matlb 960.8 for NPSS
mdotfan = BPR*mdotc; % Calculate Fan mass flow
mdot0 = mdotfan + mdotc; % Total Engine Inlet Airflow

%%%%%%% Station 2 and 3 Compressor Inlet and Exit
%%%%%%%%%%%%%%%%%%%%%%
tau_a = 8; % Thermal Limit Parameter, See definition in Burner Section
%pic = 40;
%Compressor Pressure Ratio: From Farohki, equation 4.74 page 161
pic = ((sqrt(tau_a)/(1+((g-1)/2)*M0^2)))^(g/(g-1)); %
etac = 0.9; % Compressibility Efficiency factor of the Compressor
rec = .995; %Inlet Recovery
Pt2 = Pt0*rec ;
Tt2 = Tt0;
Pt3 = Pt2*pic;
Tt3 = Tt2*(1+((1/etac)*((pic^((g-1)/g))-1)));
%%%%%%% Station 13 and 19 Fan Properties
%%%%%%%%%%%%%%%%%%%%%%%%%%%%%%

pifan = 1.3; % CHANGE THIS VALUE EVERY ITTERATION
% Using a Typical Fan value between 1.276-1.4
Pt13 = Pt2*pifan; %
Pt19 = Pt13*.95; %Account for a Small pressure loss across the Fan
tau_r = Tt0/T0;
tau_fan = pifan^((g-1)/g);
Tt13 = Tt2*tau_fan; %
V19_a0_fan = sqrt((2/(g-1))*((tau_r*tau_fan)-1));
P19 = Pt19/((1+(g-1)/2)^(g/(g-1)));
M19 = (((Pt19/P19)^((g-1)/g))-1)/((g-1)/2);
T19 = Tt13/((Pt19/P19)^((g-1)/g));
a19 = sqrt(g*R*T19);
V19 = a19*M19;
%%%%%%% Station 4 Burner Exit/Turbine Inlet
%%%%%%%%%%%%%%%%%%%%%%%%%%
g_t = 1.33; %Ratio of specific heats for the Turbine
g_c = g; %Ratio of specific heats for the compressor is the same as air
cpt = (g_t/(g_t-1))*R; % Metric Unit value should be ~1156
cpc = (g/(g-1))*R; % Metric Unit value should be ~1004
eta_b = .999; %Burner efficiency
% 0.95 for matlab 0.999 for NPSS
pib = 0.96; % Pressure Ratio Across the burner
% 0.95 for matlab 0.96 for NPSS
hpr = 120070.45; % [kJ/kg] FOR LH2  120070.45 KJ/kg
```

```
% for JET A 18550 BTU/lb=43147 KJ/Kg
Pt4 = Pt3*pib; %
%Now we need to set the "Thermal Limit Parameter" IE Turbine Temp Limit
% tau_a = ht4 / h0 % This is the definition of the Thermal Limit
Parameter
tau_a = 8; %This can be adjusted and is a driving factor in Engine
% Performance
% tau_a of 8 means Tt4 is ~1600 K if T0 is 233k
Tt4 = (cpc*T0*tau_a)/cpt; % This becomes a constant Temp Limit for all
% BPR's
f = (cpt*Tt4 - cpc*Tt3)/(hpr*10^3*eta_b - cpt*Tt4); %Need to convert
hpr
% from kJ to J with 10^3. Realize that fuel to air ratio becomes
constant
% as well.
mdot4 = mdotc*(1+f); % This is the core air flow and fuel flow
mdotfuel = f*mdotc;
%%%%%%% Station 5 Turbine Exit
%%%%%%%%%%%%%%%%%%%%%%%%%%%%%%%%%%%%%%%%%%%%
eta_m = .99; % Mechanical efficiency of the Turbine
eta_t = .936; % Flow efficiency of the turbine
%Energy Balance across the Turbine for Tt5.
Tt5 = Tt4 - ((cpc*(Tt3-Tt2) + BPR*cpc*(Tt13-Tt2))/((1+f)*cpt*eta_m));
Pt5 = Pt4*((Tt5/Tt4)^(g_t/(eta_t*(g_t-1))));
%%%%%%% Station 9 Core Exit
%%%%%%%%%%%%%%%%%%%%%%%%%%%%%%%%%%%%%%%%%%%%
% Assuming an Ideal expansion through the Nozzle
Pt9 = Pt5; %Assume Ideal Nozzle
Tt9 = Tt5; %Station 9 we assume same as turbine exit
P9 = P0; % Assume ideally expanded
%%Assume the Core is Choked for Cruise Condition IE M = 1
M9 = sqrt((((Pt9/P9)^((g-1)/g))-1)*(2/(g-1)));
T9 = Tt9/(1+(g-1)/2*M9^2);
mdot9 = mdot4;
V9 = M9*sqrt(g*R*T9);
V9_a0_core = V9/a0;
% Thrust contribution from the Core ONLY
cfg = 1; % Nozzle coefficient
Fgcore = mdot9*gc*V9*cfg;
%%%%%%% Overall Engine Thrust
%%%%%%%%%%%%%%%%%%%%%%%%%%%%%%%%%%%%%%%%%%%%
%Specific Thrust
Fn_mdot = (a0/(1+BPR))*(V9_a0_core - M0+BPR*(V19_a0_fan - M0)); % N/m/s
%Net Thrust
Fn = (Fn_mdot * mdot0)*.224809; %lbf (converting from Newton to lbf)
Fn_Metric = (Fn_mdot * mdot0); %Newtons or kg(m/s^2)
% Thrust Specific Fuel Consumption
tsfc = mdotfuel / Fn_Metric; % kg/N/s
```

```
tsfc_english = ((mdotfuel*2.20462) / Fn)*3600 ; % lb/lbf/hr (converting
kg
% to lbm and seconds to hour)
end
```

3rd order Polynomial Fit Sample Code and Data

```
close all; fclose all; clear; clc;
Xvars = [1.276 1.3 1.32 1.34]';
Yvars = [30.1987 29.8607 29.0687 27.9744]';
P = polyfit(Xvars,Yvars,3)
% saveas polyfit.fig
```

Table 15: Coefficients of the 3rd order polynomial fit

Poly fit coefficent for Jet A fuel				
Exponent	3	2	1	0
BPR poly	2787.214	-11346	15342.22	-6866.47
TSFC poly	-37.8664	155.7774	-212.636	96.77847
Poly fit coefficent for LH2 fuel				
Exponent	3	2	1	0
BPR poly	3157.019	-12879.7	17451.54	-7826.47
TSFC poly	-8.75947	37.0625	-51.8065	24.11017

Appendix B: Initial Estimates

The table below gives the initial estimates of the important design parameters.

Variable Name	Description	Change or Constant	Scaler	Current Setting	Actual	Check												
InletStart.W_in	Mass flow into the engine	Change		820.921	820.921		612.633	379.249	350.076	320.903	291.73	262.557	233.384	204.211	175.038	145.865	116.692	87.519	58.346
InEng.Fl_O.Aphy	Physical Area	Change	1.00553617	7174.4	7174.4	7174.4	5356.377751	3319.20684	3064.56048	2809.91411	2555.26775	2300.62139	2045.97502	1791.32866	1536.68229	1282.03593	1027.38957	772.743203	518.09684
InEng.Afs	Free Stream Area	Change	0.89794952	6209.5	6406.78	6406.78	4783.275792	2964.07058	2736.66993	2509.26928	2281.86863	2054.46798	1827.06733	1599.66668	1372.26603	1144.86538	917.464726	690.064075	462.663424
ratio_Aphy_Afs																			
Fan.Fl_O.Aphy	Physical Area	Change	1.00385429	7162.4	7162.4	7162.4	5347.418601	3313.65509	3059.43465	2805.21421	2550.99377	2296.77334	2042.5529	1788.33246	1534.11202	1279.89158	1025.67114	771.450703	517.230264
ratio																			
SplitFan.BPRdes	Design BPR	Change		23.742	27.1394	27.1394	20	12	11	10	9	8	7	6	5	4	3	2	1
SplitFan.Fl_O2.Aphy	Bypass Physical Area	Change		6872.94	6872.9	6872.9	5064.887212	3038.93233	2785.68797	2532.44361	2279.19925	2025.95488	1772.71052	1519.46616	1266.2218	1012.97744	759.733082	506.488721	253.244361
SplitFan.Fl_O1.Aphy	is the same as Duct2 Aphy	Constant		292.4	262	262	262	262	262	262	262	262	262	262	262	262	262	262	262
Total Internal Area		Calling Cons		7165.34	7134.9	7134.9	5326.887212	3300.93233	3047.68797	2794.44361	2541.19925	2287.95488	2034.71052	1781.46616	1528.2218	1274.97744	1021.73308	768.488721	515.244361
Duct17.Fl_I.MNdes	Mach	Constant		0.45	0.45		0.45	0.45	0.45	0.45	0.45	0.45	0.45	0.45	0.45	0.45	0.45	0.45	0.45
Duct17.Fl_O.Aphy	Physical Area	Change	1.00513611	6977.61	6908.2	6908.2	5090.901052	3054.54063	2799.99558	2545.45053	2290.90547	2036.36042	1781.81537	1527.27032	1272.72526	1018.18021	763.635158	509.090105	254.545053
NozSec.CdTh_in	Nozzle Throat Discharge Coeff	Constant		1	1		1	1	1	1	1	1	1	1	1	1	1	1	1
NozSec.Cfg_in	Nozzle Exit Gross Thrust Coeff	Constant		0.9975	0.9975	0.99750388	0.9975	0.9975	0.9975	0.9975	0.9975	0.9975	0.9975	0.9975	0.9975	0.9975	0.9975	0.9975	0.9975
NozSec.Ath	Nozzle Throat Area	Change	0.67507893	4746.8	4639.75		3419.198656	2051.51919	1880.55926	1709.59933	1538.6394	1367.67946	1196.71953	1025.7596	854.799664	683.839731	512.879798	341.919866	170.959933
NozSec.Vactual	Nozzle Exit Velocity	Constant		975.7	980.8		980.8	980.8	980.8	980.8	980.8	980.8	980.8	980.8	980.8	980.8	980.8	980.8	980.8
NozSec.Fg	Gross Thrust	Change		24436.7	25256.1		18222.52032	10933.5122	10022.3862	9111.26016	8200.13415	7289.00813	6377.88211	5466.7561	4555.63008	3644.50406	2733.37805	1822.25203	911.126016
NozSec.Fgideal	Ideal Gross Thrust	Change		25256.1	25319.1	25319.3985	18268.11973	10960.8718	10047.4659	9134.05987	8220.65388	7307.24789	6393.84191	5480.43592	4567.02993	3653.62395	2740.21796	1826.81197	913.405987
NozSec.Fl_Th.MN	Throat Mach	Constant		1	1		1	1	1	1	1	1	1	1	1	1	1	1	1
NozSec.Fl_O.MN	MN at exit	Constant		1	1		1	1	1	1	1	1	1	1	1	1	1	1	1
NozSec.PR	Pressure Ratio	Constant			2.033		1.914	1.914	1.914	1.914	1.914	1.914	1.914	1.914	1.914	1.914	1.914	1.914	1.914
Perf.myFg	Total Gross Thrust	Change			25993.6		18960.02032	11671.0122	10759.8862	9848.76016	8937.63415	8026.50813	7115.38211	6204.2561	5293.13008	4382.00406	3470.87805	2559.75203	1648.62602
OPR	55																		
SplitFan.Fl_O1.W	29.173																		
T4	3150																		
Bypass Fnet				772508.5236	776546.438														
Core Fnet				40147.8826	23160.4447														
NozPri.Vactual				1376.2	793.9														
NozPri.Fg				1476.3	737.5														
					25993.6														
Gross Thrust				22256.97124	25464.9134		18960.02032	11671.0122	10759.8862	9848.76016	8937.63415	8026.50813	7115.38211	6204.2561	5293.13008	4382.00406	3470.87805	2559.75203	1648.62602

Appendix C: Example NPSS Input File

Example input file used in NPSS are given here. The input file consists of the changing variables from the initial estimate Table. Shown here is .inp file for *BPR* 10. Notice the commented out (//F_{gross}) value is the one obtained from the initial estimate (see Table above). The actual gross thrust value that was able to give us the desired *BPR* level of 10 was 12030.42 lbf and it was achieved through fine tuning.

```
InletStart.W_in          =    320.903;
InEng.Fl_O.Aphy          =    2809.914113;
InEng.Afs          =    2509.269283;
Fan.Fl_O.Aphy            =    2805.214213;
SplitFan.BPRdes          =    10;
SplitFan.Fl_O2.Aphy =    2532.443606;
Duct17.Fl_O.Aphy    =    2545.450526;
NozSec.Ath          =    1709.599328;
NozSec.Fg           =    9111.260162;
NozSec.FgIdeal           =    9134.059867;
//Fgross            =    9848.760162;
Fgross              =    12030.42;
```